Department of Molecular Science and Nanosystems

Ca' Foscari University

Departamento de Biologia

Universidade de Aveiro

Master thesis

Gadolinium as an emerging pollutant: a review on its occurrence and impacts in aquatic ecosystems

Relators: Dr. Stefania Chiesa, Prof. Rosa Freitas

Student name: Giacomo Trapasso

Student number: 857194

Academic year: 2019/2020

Abstract

Rare earth elements (REEs), despite their name, are highly extracted and widely used metals. Thanks to their unique properties, such as ideal magnetic behaviour and sharply defined energy states, REEs are a strategic resource for many economic sectors such as energetic, nuclear, industrial, medical and digital technology. Gadolinium (Gd) is one of the most commercially exploited REEs, especially in the biomedical field where it is chelated with organic molecules and used as contrast agent in magnetic resonance imaging (MRI). Its wide employment enhances the risk for this element to be potentially released into the environment, in particular into rivers, lakes and coastal areas through industrial wastewaters or through exhausted devices. This scenario may increase the possible risks of contamination for the aquatic environments worldwide. For this reason, in this thesis, a literature review was performed with the aim to identify the Gd concentrations both in seawater and freshwater as well as in sediments and in biological matrices. In addition, information on the speciation of this pollutant in the environment is discussed, in order to understand its main chemical forms present in waters and sediments. Seawater and freshwater invertebrates and in particular bivalve species, due to their benthic ecology and filter-feeding behavior, are particularly exposed to environmental contaminants and thus potentially affected by REEs exposure in their natural environments. However, little is known about the biochemical and physiological responses of this group of organisms to REEs and, in particular to Gd exposure. Therefore, in this thesis the biochemical and physiological response caused by Gd exposure and its possible bioaccumulation in different aquatic invertebrate species is also discussed. A comparison among studies already published in literature is performed, collecting information on biomarkers activity, bioaccumulation mechanisms and physiological responses after Gd exposure in different species.

INDEX

1. Introduction

1.1 Rare earth elements (REEs): general properties and applications

Rare earth elements (REEs), as defined by the International Union for Pure and Applied Chemistry (IUPAC), integrate a group of 17 chemically similar elements comprising about 17% of all naturally occurring elements (Klinger, 2015). REEs include scandium (Sc), yttrium (Y) and 15 lanthanides: lanthanum (La), cerium (Ce), praseodymium (Pr), neodymium (Nd), promethium (Pm), samarium (Sm), europium (Eu), gadolinium (Gd), terbium (Tb), dysprosium (Dy), holmium (Ho), erbium (Er), thulium (Tm), ytterbium (Yb), and lutetium (Lu) (Gwenzi et al., 2018) (Table 1).

Table 1. List of all rare earth elements (Kumari et al., 2015).

Atomic number (Z)	Name	Symbol	Natural abundance on Earth (ppm)
21	Scandium	Sc	22
39	Yttrium	Y	33
57	Lanthanum	La	30
58	Cerium	Ce	60
59	Praseodymium	Pr	6.7
60	Neodymium	Nd	27
61	Promethium	Pm	10^{-18}
62	Samarium	Sm	5.3
63	Europium	Eu	1.3
64	Gadolinium	Gd	4.0
65	Terbium	Tb	0.7
66	Dysprosium	Dy	3.8
67	Holmium	Ho	0.8
68	Erbium	Er	2.1
69	Thulium	Tm	0.3
70	Ytterbium	Yb	2.4
71	Lutetium	Lu	0.4

A general classification divides lanthanides into two groups: light rare earths (LRE - from La to Eu) and heavy rare earths (HRE - from Gd to Lu and Y). Sc, as the lightest REE, is not similar to either LREEs or HREEs, therefore, it is not included in none of the two classes (Atwood, 2012). The classification is based on the electron configuration of each element (electron filling of the 4*f* orbitals), which determines how they interact with other compounds. Light lanthanides are considered more soluble than heavy ones (Sneller et al., 2000), but there is no worldwide accepted definition of which lanthanide belongs to which group.

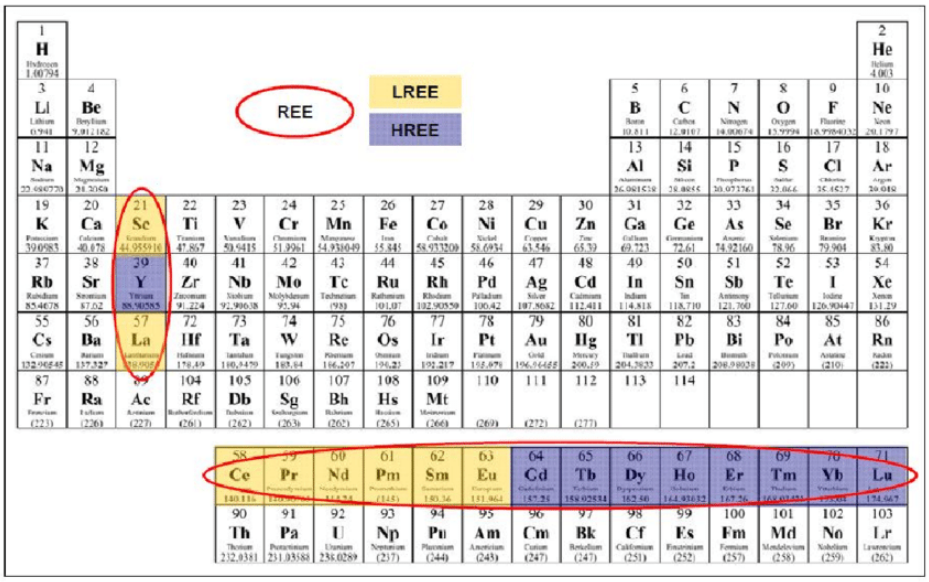

Figure 1 *- Light rare earth (LREs) and heavy rare earths (HREs) elements in the periodic table (Öhrlund, 2011).*

Rare earth elements are distributed broadly in the Earth's crust in concentrations ranging on average between 150 and 220 ppm (Kamenopoulos et al., 2016). These elements are called “rare” not because of their abundance, which is higher than those of gold or copper, but due to the fact that they are typically dispersed in ores rather than in the native form of aggregates or nuggets (as in the case of gold or copper) (Goodenough et al., 2016; Zepf, 2015). Despite the large amount of REEs, which in 2018 were estimated to be around 120 million tons (Manchen et al., 2019), the supply of these elements is restricted to only a few mining fields (Chakhmouradlan and Wall, 2012). The largest mining districts are situated in Asia (Manchen et al., 2019), among which China has the most abundant REE reserves (Shen et al., 2017; Zhou et al., 2016). Not only China has the most extensive quantity of REEs, it also has advanced processing technologies and rare earth metals production facilities. China’s rare earth mining production quota is around 120 000 tons/year, while the total world production is 170 000 tons/year (Manchen et al., 2019; Zhou et al., 2016).

The unique properties of REEs, such as ideal magnetic behaviour and sharply defined energy states, made them a strategic resource in nowadays economy (Migaszewski and Gałuszka, 2015). In fact, REEs are employed in many important sectors such as the ordinary (lighter, flints, fluorescent lamps), high-tech (batteries, lasers, super-magnets) and futuristic (high-temperature superconductivity, information storage, conservation and transport of energy) fields (Anastopoulos et al., 2016). In addition, they represent key elements (or components) of modern technologies, especially in the fields of environmental protection, medical applications, energy, nuclear industry and digital technology. Moreover, they constitute an integral part of many of today's electronic devices, serving as magnets, catalysts, superconductors, medical and agricultural products (US-EPA, 2012; Li et al., 2013; Zhang et al., 2014; Zhang et al., 2015).

The wide use of REEs in numerous industrial fields enhances the risk for these elements to potentially reach the aquatic environments (Khan et al., 2017), thus increasing the possible threats of contamination worldwide. Bau and Dulski (1996) were among the first ones to correlate the rising levels of REEs in aquatic environments with anthropogenic activities, revealing in particular a positive correlation between Gadolinium (Gd) concentrations and riverine inputs from densely industrialized areas. Their occurrence in the aquatic ecosystems is thus expected, in particular through wastewater and industrial emissions, surface run-off and atmospheric deposition (Kulaksız and Bau, 2011; Hatje et al., 2016). As a result of this increasing contamination, REEs are currently considered as "emerging pollutants" since their impacts for the aquatic fauna and flora are still poorly documented. A better understanding of their biogeochemical behavior and toxicological effects is required: little is known about the biochemical and physiological responses of marine and freshwater species to REEs.

In this article we will focus our attention on one of the most commercially exploited REEs, Gd, and its effects on aquatic wildlife.

1.2 Gadolinium: general properties and applications

Gadolinium is a soft, shiny, ductile, silvery metal belonging to the lanthanide group of the periodic table (Hron et al., 2009). Unlike the other REEs, this metal is relatively stable in dry air. However, it is oxidized quickly in moist air forming a black and thin film of Gd_2O_3 on its surface. Moreover, Gd slowly reacts with water and its complexes are typically dissolved in acids. For this reason, Gd is usually found in dissolved form, while other REEs of anthropogenic origin (such as La and Sm) exist in colloidal or nanoparticulate form according to the pH, temperature and to the types of ligands

involved (Gwenzi et al., 2018). For example, nitrates, chlorides and sulfates REEs species are soluble in water, while their carbonates, phosphates and hydroxides forms are not (Wells and Wells, 2001; Gonzalez et al., 2014). Gadolinium, in addition, is the only lanthanide that has a ferromagnetic behaviour near room temperature, but above 293 K (Curie point - T_c) the element becomes a very strong paramagnet (Dan'kov et al., 1998).

Gadolinium is one of the most abundant REE, with a concentration in the Earth's crust around 6.2 mg/kg (Greenwood and Earnshaw, 1997). In addition, it cannot be found as free element in nature, but it is contained in many minerals (i.e bastnasite, laterite clays, monazite, and loparite) (Pecharsky and Gschneidner Jr., 2019) . The main mining areas are located in China, USA, Brazil, Greenland, India, and Tanzania with reserves expected to exceed one million tonnes (Emsley, 2011; Rogowska et al., 2018).

Figure 2 *– Gadolinium sample.*

Table 2. Chemical properties of gadolinium (Gd).

Gadolinium	
Atomic number	64
Atomic mass	157.25 g*mol^{-1}
Electronegativity	1.1
Density	7.9 g*cm^{-3} at 20°C
Melting point	1313 °C

Gadolinium is mainly employed in medicine as a contrast agent in magnetic resonance imaging (MRI) (Telgmann et al., 2013), but it has also many uses in different industrial applications, such as control rods for nuclear reactors and nuclear power implants, garnets for microwave and phosphorous for colour TV tubes. Metallic Gd is rarely used as a metal itself, but its alloys are exploited to manufacture magnets and electronic components, such as recording heads for video recorders in compact disks and in computer memory (Rogowska et al., 2018). The wide usage of Gd opened a debate and raised concerns about its contamination into the environment. In recent years (2013), in Germany, approximately 12 tons of Gd/year were used for biomedical purposes and then released via sewage systems into the environment (Cyris, 2013). Even if diagnostic forms of Gd are not toxic for living organisms, during processes occurring in the wastewater treatment plants,

modifications of Gd complexes might occur and consequently toxic compounds may be released in the aquatic environments (Cyris, 2013).

1.2.1 Gadolinium chelates as contrast agents in magnetic resonance imaging (MRI)

Gadolinium proprieties highlighted in the previous section, made this element the first and the most often employed magnetic resonance imaging contrast agent starting from the 1980s, due to its highly paramagnetic proprieties (Runge, 2018; Telgmann et al., 2013).

Gadolinium-containing MRI contrast agents are constituted by aqueous solutions that, once injected into the patient, allow a detailed view of various parts of the body, improving the image quality and permitting a more accurate picture to be observed (Raju et al., 2010). For this purpose, Gd ions are bound to other molecules, in order to decrease or even nullify their toxicity, however maintaining the water-solubility characteristics. This process is called chelation. Chelating agents can be either made by linear or macrocyclic molecules. Linear chelates are less stable than the macrocyclic ones. Linear chelates can further be divided into 2 groups: non-ionic and ionic, with the former one less thermodynamically stable (Figure 3) (Runge, 2018).

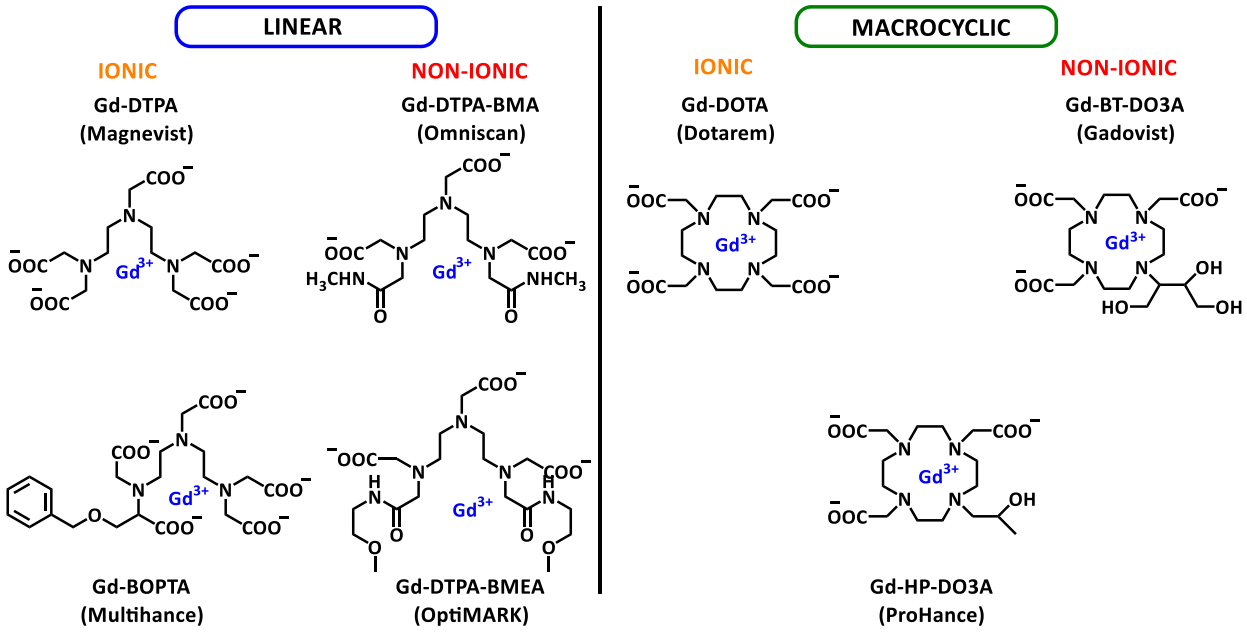

Figure 3 *- Structure of some Gd-based MRI contrast agents and their respective trademarks.*

Nevertheless, even if in most cases the complexation of the Gd ion reduces dramatically its toxicity, Kümmerer and Helmers (2000) study reported that the level of Gd in MRI patients' urine may reach 350 mg/L daily after the medical exam and 7 mg/L after 39 days. These concentrations may cause

the appearance of severe diseases, such as nephrogenic system fibrosis (NSF) as well as accumulation in patients' brain, bones and kidneys (Idee et al., 2006). Histological examination showed pathological results such as diffuse ulcerative calcific atherosclerosis, patchy myocardial necrosis and fibrosis, central venous congestion of the liver as well as calciphylaxis and necrotic skin. The average time between the diagnosis of NSF and death was reported to be 112 days for patients with a median age of 55 years (Clases et al., 2018). Nephrogenic system fibrosis causes characteristic symptoms like thickening and hardening of the skin. This disease has been associated prior to the administration of Gd chelates, with higher incidence in patients affected with renal inefficiency (Grobner and Prischl, 2007; Mendichovszky et al., 2007). Even if this cutaneous disease is only observed for patients with chronic or acute kidney failure, the evaluation of many studies indicated that in most cases the administration of Gd complexes with linear ligands led to NSF (Belin and Van Der Molen, 2008; Thomsen and Marckmann, 2008). However, it must be remarked that only few numbers of NSF cases have been tracked back to the administration of Gd complexes. For these reasons, the pathogenesis of NSF due to these compounds can be considered as unclear (Telgmann et al., 2013).

Due to these findings, further analytical methods for the detection of this metal in the organism and in the environment must be developed (Telgmann et al., 2013). All these Gd-chelated compounds are applied orally or intravenously at a dose of about 0.12 mmol Gd complex per kg of body weight, which corresponds roughly to 1.2 g of Gd per person (with an average body mass of 65 kg) (Möller et al., 2003). It is estimated that 25–30% of all MRI investigations are performed with the help of contrast agents, resulting in about 20 million applications per year worldwide (Cyris, 2013). Clinical studies revealed that Gd complexes are excreted in non-metabolised form by the patient within few hours. After excretion, Gd complexes enter the hospital sewage system, contaminating surface and river waters (Raju et al., 2010).

1.2.2 Gadolinium complexes dechelation process

A possible reason for the toxicity of Gd complexes could be the dechelation mechanism. This process involves the specific release of the Gd ion which can occur *in vivo* with the less stable complexing agents. In living organisms, only Zn^{2+} can substitute a significant amount of Gd^{3+} since its concentration in blood is relatively high (55– 125mM) and its association towards EDTA, DTPA or DOTA (used as chelating ligands in most of the Gd-based MRI contrast agents) is only about four orders of magnitude lower than for Gd^{3+} ions. This process is called transmetallation (Scheme 1) (Laurent et al., 2010; Runge, 2018). Other potential challengers exist but can be neglected: copper

ions are present but in small amounts (1–10 mM), calcium ions have a low affinity constant to organic ligands and iron ions are not available for transmetallation since they are strongly bound to ferritin and haemoglobin. Therefore, the stability of Gd complexes in the presence of Zn^{2+} is an important issue. Transmetallation induces a release of Gd cations and a possible depletion of the endogenous zinc ion subsequent to its renal elimination as a hydrophilic complex (Laurent et al. 2010).

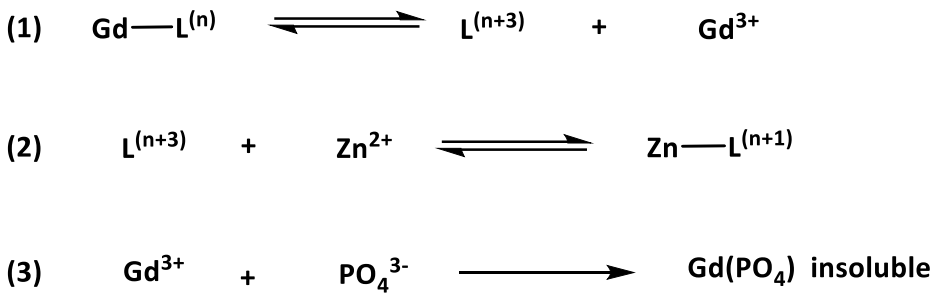

Scheme 1 *– transmetallation process between Gd^{3+} and Zn^{2+} ions*

This process has been studied in recent years as safety concerns increased regarding the least stable gadolinium-based contrast agents (GBCAs) (Runge, 2018).

The overall mechanism of Gd toxicity is based on the coordination of the metal to donating groups in bio-macromolecules (e.g. proteins). Such coordination causes a malfunctioning of the cell membrane and/or of the enzyme activity (Rogowska et al., 2018). In fact, Gd^{3+} cation presents an ionic radius of 107.8 pm, which closely resembles the one of Ca^{2+} (114 pm) (Sherry et al. 2009). Due to this similarity, free Gd behaves as an inorganic blocker of many types of voltage-gated Ca channels at nano- to micro-molar concentrations. In addition, it inhibits physiological processes which depend upon Ca^{2+} influx (causing lack in contraction of smooth, skeletal and cardiac muscles, transmission of nervous influx or blood coagulation) as well as the activity of some enzymes. Nevertheless, chelation of Gd^{3+} with suitable ligands reduces dramatically its acute toxicity (Bellin and Van Der Molen, 2008; Rogowska et al. 2018).

1.3 Literature selection

As mentioned in the previous paragraphs, Gd employment in medical and technological field started relatively late, around 1980s, with a pronounced increase in its use only in the last two decades. For this reason, scarce literature exists on this topic and consequently few studies have been performed

on the behaviour that this pollutant can have in the environment and inhabiting wildlife. Nevertheless, an increasing number of researchers have focused their attention on the possible toxic effects of this metal and of their derivatives, performing both laboratory and *in-situ* experiments.

For the present thesis, the bibliographic search was carried out exploiting WoS (Web of Science), Google Scholar, Scopus and PubMed databases, covering all years from 1980s up to June 2020, using specific topics and/or keywords such as: ‘‘gadolinium effects on marine and freshwater invertebrates’’ and ‘‘gadolinium environmental effects’’ combined with (a) ‘‘biochemical effects’’; (b) ‘‘bioaccumulation patterns’’; (c) ‘‘biomarkers’’; (d) ‘‘gene regulation’’ and (e) ‘‘metal uptake”. The bibliographic search has been focused on bioaccumulation as well as on the analysis of biochemical and physiological effects of Gd on aquatic invertebrate species, since they are particularly exposed to environmental contamination.

A schematic flow diagram (modified from Chiesa et al., 2019) is provided in Figure 4, to illustrate the pipeline of paper search along with selection and processing. For this study, data have been obtained from around 120 scientific papers, comprising analysis on different invertebrate species and various marine and freshwater environments worldwide.

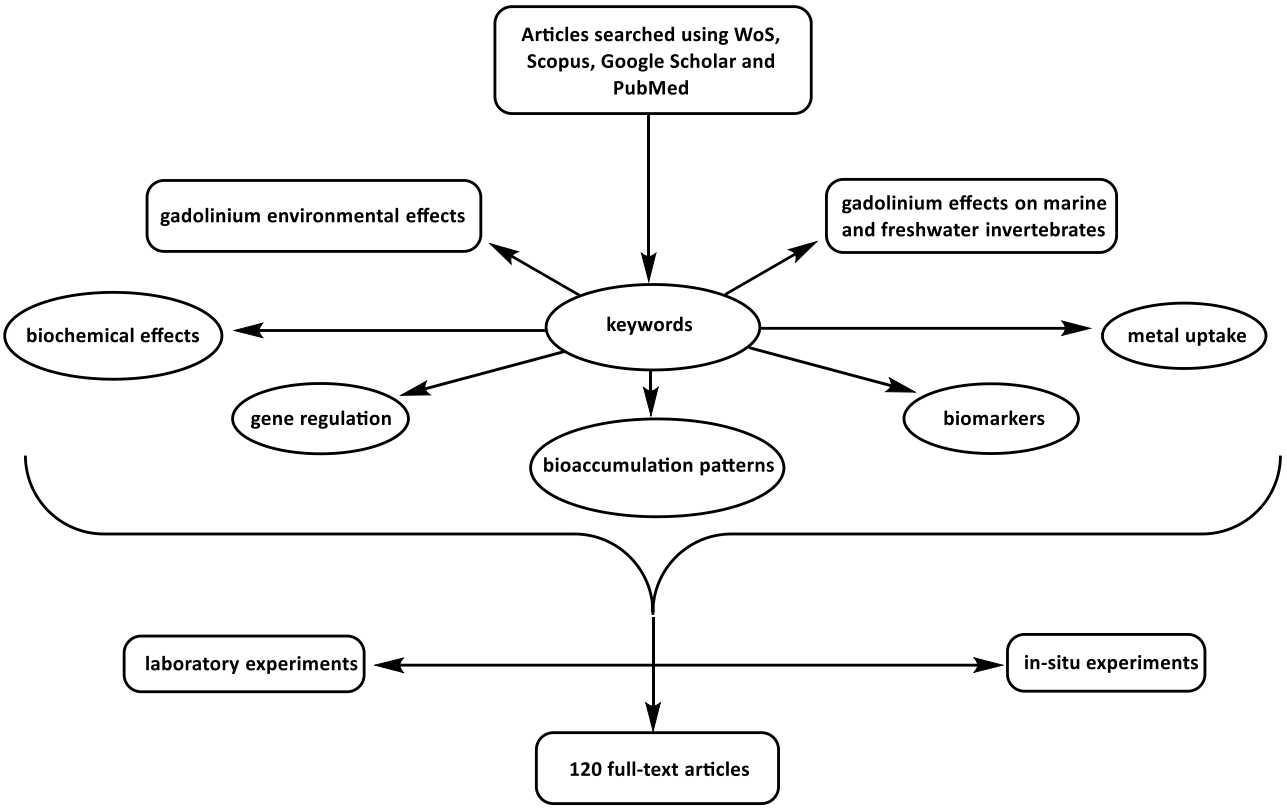

Figure 4 *- Schematic flow diagram representing the pipeline of paper search.*

2. Gadolinium quantification in aquatic environments

2.1 Analytical methods for total Gadolinium detection

Concentrations of Gd in water solutions can be determined by using spectrometric techniques such as atomic absorption spectrometry (AAS), inductively coupled plasma atomic emission spectrometry (ICP-AES), X-ray fluorescence (XRF) and inductively coupled plasma mass spectrometry (ICP-MS) (Raju et al., 2010).

2.1.1 Atomic absorption spectrometry (AAS)

Atomic absorption spectrometry (AAS) is a technique in which, after the vaporization of the sample, the element of interest is atomized at high temperatures in a cell called “atomizer”. The type of atomizer defines the two main AAS-based analytical techniques:

- flame AAS (FAAS) that provides analytical signals in a continuous fashion;
- electrothermal AAS (ETAAS) delivering analytical signals in a discontinuous mode (2–4 min per sample).

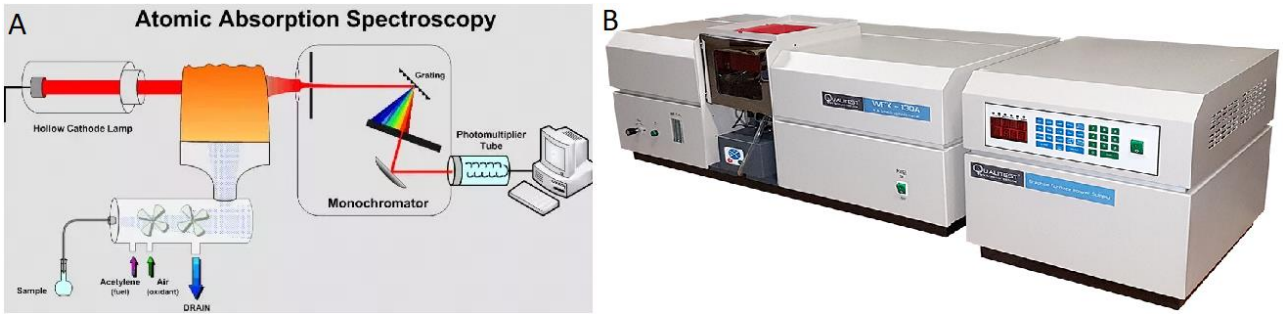

Figure 5 *– A) Atomic Absorption Spectrometry (AAS) diagram[1]; B) Atomic Absorption Spectrometer (AAS) machinery[2].*

Free gaseous atoms obtained in this way absorb electromagnetic radiation at a specific wavelength emitted from a light source (typically a hollow cathode lamp containing the element to be measured) to produce a measurable signal. The absorption signal is proportional to the concentration of those free absorbing atoms in the optical path. After the atomization process, liquid (or dissolved) samples are easily introduced into the analyser, as an aerosol in the case of FAAS or as well-defined low microliter volumes in ETAAS. Furthermore, the coupling of hydride generation and cold vapour methods allow the introduction of analytes in the atomizer as a gas phase. Also, especially in ETAAS, direct elemental analysis of solids without previous dissolution is feasible (Fernández et al., 2019; Cheremisinoff, 1996). A diagram of this analytical process has been depicted in Figure 5.

2.1.2 Inductively coupled plasma atomic emission spectrometry (ICP-AES)

Inductively coupled plasma atomic emission spectrometry (ICP-AES) technique is useful for the determination of a wide variety of elements in geologic materials, but it can be also used to quantify the mass percentage of the metals in metal/polymer nanocomposites (Pramanik and Das, 2019). It offers better precision, superior limit of detection for most elements and faster rates of analysis for multiple-element samples compared to atomic absorption spectrometry (AAS). A typical instrumental scheme is reported in Figure 6.

[1] https://www.scienup.com/product-page/atomic-absorption-spectroscopy-aas;
[2] https://www.worldoftest.com/atomic-absorption-spectrometer

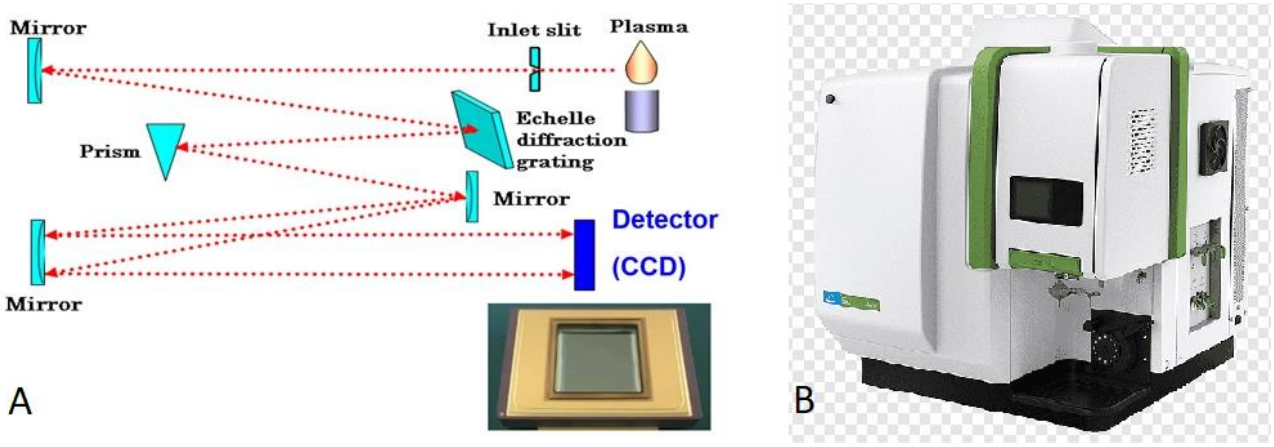

Figure 6 *– A) Inductively coupled plasma atomic emission spectrometry (ICP-AES) diagram[3]; B) Inductively coupled plasma atomic emission spectrometry (ICP-AES) machinery[4].*

The analyte-containing solution is firstly nebulized. The resulting aerosol is then injected into the plasma which consists of Ar ions and free electrons and produces excitations temperatures of approximately 6000 K. It gives a very high signal-to-noise ratio for spectral lines of over 50 elements. Then, due to the high temperatures, the sample is melted, vaporized, atomized and ionized. Finally, the plasma excites the outer-shell electrons of the free atoms and ions of the elements in the sample. The relaxation of an excited atom is accompanied with the emission of a photon of light. The energy of this photon is characteristic of the atomic energy level transition and thus specific for each element. Finally, the grating disperses the photons according to their energy or wavelength (λ). The intensity of a selected discrete λ is measured by a photomultiplier tube placed behind an exit slit giving the final spectrum as an output (Baedecker, 1770).

2.1.3 X-ray fluorescence (XRF) spectrometry

X-ray fluorescence (XRF) is based on the irradiation of a sample by a primary X-ray beam. The individual atoms hereby excited, emit secondary electrons that can be detected and recorded in a spectrum. The peaks of such spectrum are characteristic of the individual atoms, that is, of the respective elements of the sample. In this way, the reading of an XRF spectrum gives the elemental composition of the sample. This method is fast and can be applied universally to a wide variety of samples containing heavy metals atoms, which must have an atomic number greater than 11. Due to its characteristics, this detection methodology plays an important role in the industrial production of materials, in prospecting mineral resources and also in environmental monitoring

[3] https://www.ssi.shimadzu.com/industry/environmental/icp-aes.html
[4] https://www.perkinelmer.com/it/product/avio-500-oils-configuration-n0810012

(Klockenkämper and Von Bohlen, 2015). An overall scheme of the x-ray fluorescence method is depicted in Figure 7.

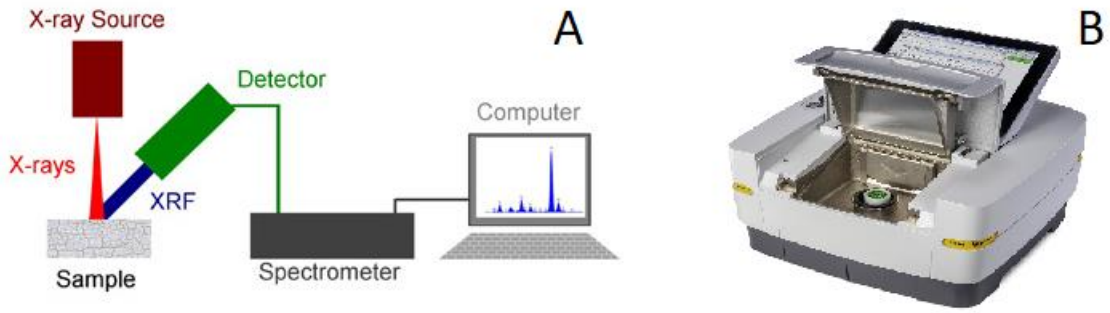

Figure 7 *– A) X-ray fluorescence (XRF) spectrometry diagram[5]; B) X-ray fluorescence (XRF) spectrometer machinery[6]*

2.1.4 Inductively coupled plasma mass spectrometry (ICP-MS)

Inductively coupled plasma (ICP-MS), the most widely applied plasma source mass spectrometry, has played and still plays an important role in many fields of applied science and research. Nowadays, ICP-MS is routinely employed in geochemistry, environmental and life sciences, industries (food, chemical, semiconductor, nuclear), forensic science and archaeology. An ICP is the standard high-temperature ion source and provides temperatures of approximately 6000 K. Contrary to low-temperature ion sources for molecular ions, in a plasma all bonds are broken irrespective of their chemical bonding. Hence, the data acquired from a plasma ion source corresponds to the total content of an element in the sample. The ionic fragments generated by the ICP are then collected and analysed according to their mass-to-charge ratio (*m/z*) by the mass spectrometer (MS) (Ammann, 2007). A typical scheme of the instrument is depicted in the figure below (Figure 8).

[5] http://physicsopenlab.org/2016/02/24/diy-xrf-spectrometry/
[6] https://global-recycling.info/archives/3010

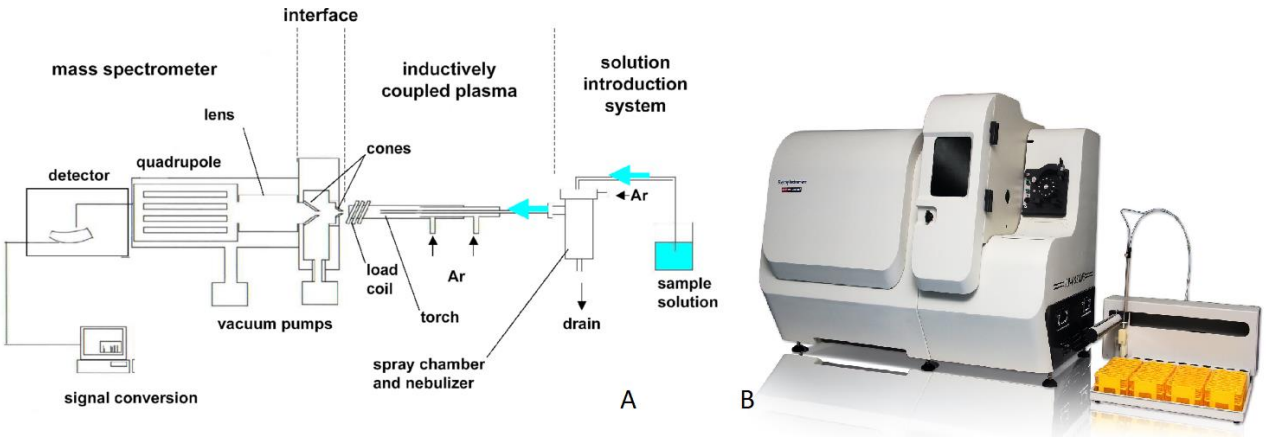

Figure 8 *– A) Inductively coupled plasma mass spectrometer (ICP-MS) diagram; B) Inductively coupled plasma mass spectrometer (ICP-MS) machinery (Gilstrap and Allen, 2009).*

2.1.5 Hydrophilic interaction chromatography (HILIC)

All the techniques reported in sections from 2.1.1 to 2.1.4 are unable to distinguish the contrast agents and the various chemical species of Gd potentially present in the sample. In particular, ICP-MS delivers solely information about the overall metal content, since all species information is lost during atomization in the ICP (Clases et al., 2018). To gather more detailed information about the Gd species, chromatographic techniques are required to separate each Gd complex in order to detect them individually. Nevertheless, compounds with hydrophilic properties, like metal ion solutions, are poorly retained by reversed phase interactions. In these cases, hydrophilic interaction liquid chromatography (HILIC) has recently emerged as a powerful alternative with improved performances. In addition, considering that ICP-MS is the most sensitive detection method for trace metal concentration analyses, a combination of HILIC-ICP-MS could be suitable for the speciation and subsequent quantitative determination of Gd based contrast agents in the environment (Raju et al., 2010). On the other hand, it must be mentioned that the direct determination of REEs in seawater samples with ICP-MS is still a challenge due to the remarkable matrix effect and potential spectral interferences. In fact, a high salt content in seawater could cause various problems, among which instrument sensitivity drift and signal suppression. Moreover, in many environmental samples some coexisting elements such as barium, tin and antimony possibly bring serious spectral interference (oxides ions and hydroxides) during the ICP MS determination of some REEs (europium, lanthanum and cerium) (Pyrzynska et al., 2016).

Therefore, HILIC can be considered as a powerful analytical technique to separate polar and hydrophilic compounds, like Gd-based contrast agents, on a polar stationary phase and it is a good

alternative for all the compounds that are retained poorly on reversed-phase columns (Raju et al., 2010). Most of the recently published works use conventional nonmodified (naked) silicas as a stationary phase and a polar organic solvent (most frequently acetonitrile and sometimes methanol) containing up to 30% water (see Gama et al., 2012; Hemström and Irgum, 2006 as examples). When a hydrophilic chromatography column is eluted with a hydrophobic (mostly organic) mobile phase, retention increases with hydrophilicity of solutes (Alpert, 1990).

2.2 Total Gadolinium concentrations in rivers and coastal waters

In 1996, about 12 years after their first use in 1984, the presence of anthropogenic Gd was observed in German rivers (Bau and Dulski, 1996). Since then, similar observations have been reported in several countries such as France, China, the USA, Brazil, and Turkey (Zhao et al. 2007; Rabiet, 2009; Zhou et al., 2012; Barber et al., 2015; Hatje et al. 2016; Perrat et al., 2017; Parant et al., 2018; Pedreira et al., 2018; Alkan et al., 2020; Altomare et al., 2020; Pereto et al., 2020) but also in Kazakistan, Portugal, Republic of Benin and Australia (Pratas et al., 2017; Yessoufou et al., 2017; Xu et al., 2018; Rzymski et al., 2019) in much lower concentrations. Nevertheless, in this thesis, only noteworthy Gd anomalies reported among these countries will be discussed.

Moreover, the presence of anthropogenic Gd have been also detected in surface and drinking water (Birka et al., 2016a), indicating that components from the contrast agents are not removed during conventional wastewater treatment. A study about this issue showed that approximately 10% of Gd is removed during these depuration processes while only advanced WWTPs are able to remove 100% of it (Rogowska et al., 2018). Finally, Gd long environmental half-life and conservative estuarine behaviour suggest that anthropogenic Gd might be utilized as a pseudo-natural far-field tracer for truly dissolved riverine REEs input into seawater, for discharge from wastewater treatment plants as well as for sewage in river, ground and drinking water (Kulaksız and Bau, 2007). In fact, the amount of anthropogenic Gd introduced into seawater via rivers is significant and produces anthropogenic positive anomalies in coastal seawater. This is observed in the southwestern North Sea, off the coast of the East Frisian Islands, where anthropogenic Gd is mostly derived from the rivers Rhine and Thames (Kulaksiz and Bau, 2007). A further proof that the positive Gd anomalies have anthropogenic origin, comes from the fact that rivers in thinly populated, non-industrialised areas in Värmland and Dalarna, central Sweden, and Hokkaido, Japan, do not show such high concentration of Gd compared to the majority of German rivers (Rhein, Elbe, Mosel Wupper, Spreeand Havel) (Bau and Dulski, 1996). Data have been depicted in Table 3.

Table 3. Concentrations of "dissolved" Gd in river and stream waters from Sweden, Japan and Germany (modified from Bau and Dulski, 1996)[a]

Sweden	**Japan**	**Germany**					
Vasterdalllven (Dalarna)	Toshibetsu (Hokkaido)	Rhein	Elbe	Mosel	Wupper	Spree	Havel
265	77.4	54.7	36.0	29.2	207	43.1	675
Gd_{SN}/Gd^{*}_{SN}[b]							
1.2	1.2	1.9	1.9	1.7	30	12.4	126

[a]Concentrations expressed in pmol of Gadolinium per Kg of water sample. [b]Gd_{SN} : shale-normalized Gd anomalies; $Gd_{SN}/Gd^{*}_{SN} = Gd_{SN}/(0.33Sm_{SN} + 0.67Tb_{SN})$.

Evidences coming from the analysis of Gd-contaminated water samples showed that these anomalies are most likely to result from the application of gadopentetic acid, $Gd(DTPA)^{2-}$ in magnetic resonance imaging (MRI), particularly employed from the 1980s. It is worth of mention that also rivers, lakes, semi-closed sea basins, and coastal seas receive riverine REEs input from industrialised, densely populated areas. This fact contributes to the spreading of the contaminant along worldwide waters (Bau and Dulski, 1996).

In addition to the environmental issues caused by this REE, it must be considered that the widespread distribution of anthropogenic Gd, proven by the various studies performed worldwide in marine and freshwaters (see sections from 2.2.1 to 2.2.6), is an example of how the increasing use of "exotic" (ultra)trace elements in high-tech processes will significantly hamper studies of the distribution and geochemical behaviour of such elements in natural systems in the future (Kulaksız and Bau, 2007).

2.2.1. Anthropogenic gadolinium in German rivers and estuaries

During 1990s in German hospital's effluents, Gd emission ranged between 2.1 and 4.2 kg/year, yielding a theoretical concentration of 8.5−30.1 μg/L (Kummerer and Helmers, 2000), while in 2013 approximately 12 tons of Gd/year, used for biomedical purposes, were released via sewage system into the environment (Cyris, 2013). Moreover, based on consumption data, the total Gd input by German hospitals was estimated to be roughly 132 kg/year in 1994. An increasing of the natural concentration of Gd in German surface waters by 0.003−0.004 μg/L is thought to result if there will be no elimination in sewage treatment plants (Kummerer and Helmers, 2000). Considering the total number of magnetic resonance imaging (MRI) apparatus used in Germany by hospitals and

practices, the annual emission has been stated between 484 kg and 1160 kg, resulting in an additional Gd concentration in German surface water of 0.011 and 0.026 µg/L, respectively (Kummerer and Helmers, 2000). Therefore, the emission of Gd compounds used in magnetic resonance imaging must be considered as one source among others of anthropogenic Gd anomaly in surface waters (Kummerer and Helmers, 2000). Even if diagnostic forms of Gd are not toxic for living organisms, during processes occurring in the wastewater treatment plants (WWTPs), modifications of Gd complexes might occur and consequently toxic compounds may be released in the aquatic environments (Cyris, 2013). Another issue that must be considered is that all major rivers in north western Germany flow into the North Sea, bringing with them positive Gd anomalies. As normally happens, a large fraction of the natural dissolved REEs in rivers is made by colloids. These colloids aggregate during mixing between freshwater coming from river effluents and seawater of estuaries (Kulaksiz and Bau, 2007). As a consequence, the dissolved REEs are partially removed from the river water together with the colloids. In marked contrast to the natural REEs, the anthropogenic Gd behaves conservatively during this estuarine mixing and transits through the estuary almost unaffected. This indicates that the speciation of anthropogenic Gd is different from that of natural Gd and suggests a long environmental half-life of the anthropogenic Gd complexes used as contrast agents (Kulaksiz and Bau, 2007).

2.2.2 Anthropogenic gadolinium in United States

Analyses performed in San Francisco Bay (SFB), US revealed a temporal increase in the Gd concentration from the early 1990s to the present (Bau and Dulski, 1996; Hatje et al., 2016). The highest Gd anomalies were observed in the southern reach of SFB, which is surrounded by several hospitals and research centres that use Gd-based contrast agents for magnetic resonance imaging. Recent increases in that usage presumably contributed to an increase in anthropogenic Gd concentrations in SFB, from 8.27 to 112 pmol/kg over the past two decades (Hatje et al., 2016). These data are in accordance with other researches which states that anthropogenic, strongly chelated, anionic Gd complexes appear to behave conservatively during the estuarine mixing and have a long environmental half-life (Kulaksız and Bau, 2013). Barber et al. (2015), instead, provided a long-term evaluation, between the years 1999 and 2009, of the occurrence of many contaminants discharged from WWTPs into streams in the Great Lakes and Upper Mississippi River Regions (Indiana, Illinois, Michigan, Minnesota, and Ohio). Among all the contaminants reported, Gd showed a positive anomaly in the Calumet WWTP effluent, situated in the highly industrialized area between the city of Chicago, Illinois and Gary, Indiana (Barber et al., 2015). These findings further

demonstrate the lack of removal of Gd through any of the WWTPs treatments employed and illustrates the potential persistence of this contaminant which can easily be associated with specific human activities, such as medical practices and in particular MRI imaging (Barber et al., 2015).
Another study performed by Altomare et al. (2020) highlighted the presence of noteworthy anthropogenic Gd concentrations in the Orlando Easterly Wetlands (OEW), located east of Orlando, Florida which is one of the largest constructed wetland treatment systems in the state. The presence of many hospitals and smaller medical facilities in this area constitute an anthropogenic source of Gd, which has been noted both in the wetland water (values ranging between 555 and 422 ng/L) and sediments (Gd_{Ant}/Gd_{Geo} ratio on average of 5.34 – see section 2.3.2 for further information). According to the data collected, the overall Gd input in this area is thought to be of approximately 25 g of Gd/day (Altomare et al., 2020).

2.2.3 Anthropogenic gadolinium in French rivers

Systematically pronounced positive gadolinium anomalies were also observed in WWTP effluents in southern and western France (Rabiet, 2009; Pereto et al., 2020). These observations have shown that Gd can be also found in wastewater drained from rural communities, not equipped with MRI facilities. Positive Gd anomalies were detected in two tributaries of the Hérault River and in some wells supplying drinking water, corresponding to an excess of anthropogenic Gd in water up to 15.4 pM (Rabiet, 2009). A monthly monitoring on one well has confirmed the persistence of Gd anomalies all along the year, suggesting a continuous wastewater contamination on this site (Rabiet, 2009). In addition, anthropogenic Gd was found in in the Mosel river, close to the WWTPs of the cities of Metz and Nancy, and in the Jalle River, near the city of Bordeaux. Analysis showed that the total amount of metal present in the water samples varied between 40 and 630 ng/L, with an estimation of the anthropogenic Gd reaching 67% of the total Gd in the former case, and between 58.0 and 132.5 ng/L with an estimation of the anthropogenic Gd between 2.8 and 86.9 ng/L in the latter one (see chapter 3.1.2 for further informations) (Perrat et al,. 2017; Pereto et al., 2020). Further studies detected strong anthropogenic Gd anomalies in the Lorraine region rivers, with noteworthy REE concentrations which reached peaks of more than 80 µg/L near the WWTPs (Parant et al. 2018). These concentrations were further diluted into the river stream and were measured to be around 10 ng/L close to the catchment areas used for drinking water (Parant et al., 2018). The high variability in the data collected, could be related to the population density, which is highly concentrated in the biggest cities where the major part of MRI examinations is performed. These

data also showed that the use of GBCAs is constantly increasing, leading to a growing associated waste discharged into river waters (Parant et al., 2018).

2.2.4 Anthropogenic gadolinium in Brazilian coastal waters

Water samples have been taken along the coast of North-eastern Brazil, near the city of Salvador, to investigate the influence of two submarine sewage outfalls on the distribution of Gd in the coastal waters (Pedreira et al., 2018). Positive Gd anomalies have been observed in most of the sampling sites, indicating the occurrence of anthropogenic Gd also in coastal waters. The highest Gd anomalies have been found in the proximity of the submarine sewage outfalls with a decreasing concentration as the distance increases from the point source (Pedreira et al., 2018). The total daily discharge of Gd has been calculated to be around 216 ± 82 g for the Rio Vermelho zone and 92.0 ± 19 g for Boca do Rio submarine outfalls, respectively. It has been estimated that in 2016 the annual emission of anthropogenic Gd by hospitals and clinics in Brazil varied between 527 kg and 5.3 tons (De Campos and Enzweiler, 2016). In particular, it was roughly estimated that a quantity between 698 and 2021 g Gd/day have been discharged into the Tropical and South Atlantic waters due to submarine outfall sewage along the coast of Brazil (Pedreira et al., 2018).

2.2.5 Anthropogenic gadolinium in Chinese rivers

A study conducted in the Shanxi Province in the North of China by Zhao et al. (2007) to determine geochemical characteristics of REEs in acid mine drainage (AMD), reported higher concentrations of REEs compared to global terrestrial water. The total concentration ranged from 54.37 to 68.80 µg/L while Gd concentration ranged between 3.18 and 4.27 µg/L. Shili River samples with AMD acts as an indicator of REEs enrichment, especially for Sm, Eu, and Gd. River water and other tributaries near mining industries showed concentration of REEs that are three orders of magnitude higher than natural river waters in Northern China (Zhao et al., 2007). In addition, in the Yellow river in Baotou, the concentration of REEs in the surface water and sediments were found to be 200 times higher than other rivers in Northern China (Zhou et al., 2012), while in the Maluan Bay, anomalies involving both LRE and HRE elements have been reported in all the water samples collected (Wang et al., 2019). Sidaosha River instead was found enriched with REEs, with 31.52 and 30.46 µg/L in suspended particles and sediments, respectively (Zhou et al., 2012). The concentration of Gd (4.55 mg/L) in river water samples was found to be lower compared to other REEs, causing also a high variability of the data collected.

2.2.6 Anthropogenic gadolinium in Turkish rivers

According to the Organisation for Economic Co-operation and Development (OECD), Turkey is listed as the first place in the world in terms of the number of applications and instruments for MRI imaging (OECD, 2015). Despite this fact, there is no research on the possible effects of this metal on the environment across the country. In the study performed by Alkan et al. (2020), Gd concentrations have been measured in water and sediment samples taken from various locations in the Ankara Stream, Turkey and its tributaries. The highest mean Gd concentration was found to be 0.347 ± 0.057 μg/L in water samples, which was one of the highest values among most rivers in the world (Alkan et al., 2020). For what concerns the Gd concentration in sediment samples, Alkan et al. (2020) found an average of 3.52 mg/kg, with no statistically significant difference between the different sampling sites. In addition, Gd concentrations measured in sediments had been found to have very high correlation values with other lanthanides (such as: Nd, Sm, Eu, Pr, La, Tb, Ho, Dy, Er, Tm). This can be considered as a sign that Gd is likely of geological origin (Alkan et al., 2020). On the other hand, the lower correlation between Gd and other lanthanides in water samples, reinforced the possibility that Gd behaves differently from the other REEs in aquatic environments and thus can be considered to be of anthropogenic origin (Alkan et al., 2020).

2.2.7 General remarks

According to what was described before, Gd can be considered as an indicator for the monitoring of anthropogenic pollution, even if there is no legal limit for REEs in natural waters. However, at the end of 2017, the European Medicines Agency (EMA) proposed to limit the use of some linear based products and to suspend some linear and macrocyclic compounds used in magnetic resonance imaging (MRI) (Alkan et al., 2020).

The results presented (see sections from 2.2.1 to 2.2.6), demonstrate that Gd anomalies have been reported in both marine and freshwaters worldwide samples, highlighting a high diffusion of this contaminant. The highest freshwaters Gd values reported have been found in France (particularly the Lorraine region), Germany, and Turkey, with concentrations reaching 80, 30.1, and 0.347 μg/L respectively. Concerning marine waters instead, very few information is available in literature. This is mainly due to the high difficulty in determining REEs in seawater due to the remarkable matrix effect and potential spectral interferences during measurement with spectrometers (ICP-MS) (Pyrzynska et al., 2016). In addition, it must be mentioned that it is difficult to differentiate the background concentration due to the geogenic processes in water. Therefore, the high oscillations

in the analytical data obtained could be indicative of an external source for this element in the waters examined (Khan et al., 2016).

2.3 Chemical speciation of gadolinium

As reported in section 1.2.1, clinical studies revealed that MRI Gd complexes are excreted in non-metabolised forms by the patients within few hours after administration. Moreover, most of the compounds are not retained in wastewater treatment plants (WWTPs) and might be released into the surface waters of rivers or lakes (Raju et al., 2010). The reason for this phenomenon can be either attributed to the high solubility of these compounds (they are not absorbed by organic particulate matter) or to their high resistance to microbial degradation (Braun et al., 2017). In this scenario, understanding which Gd chemical forms occur in the environment will help to distinguish natural from anthropogenic Gd, to achieve a better knowledge of Gd contamination and its anthropogenic and/or natural sources. In particular, it is urgent to determine the stability in seawater of the GBCAs currently used, particularly for the most widely employed macrocyclic GBCAs such as gadoterate meglumine, gadobutrol and gadoteridol, as the world consumption of these molecules is increasing. Studies on this topic would be essential for the prediction of the consequences of gadolinium pollution in coastal environments and possibly develop water treatment processes (Le Goff et al., 2019). For these reasons, information on Gd speciation are necessary for environmental and toxicity studies.

2.3.1. Methods for REEs speciation and metal mobility

Speciation can be defined as the identification and quantification of the different forms and species of the target element present in the various phases (Khan et al., 2016). Information about the physicochemical forms of the elements via speciation provides a better understanding of their corresponding mobility, pathways, toxicity and bioavailability. Chemical speciation of REEs in sediment provides not only information on the degree of pollution but also the actual environmental impact, their bioavailability, as well as their respective origins (Khan et al., 2016). In order to determine the various pollutant forms present in a sediment sample, sequential extractions must be performed. The extraction procedure employed is usually the one described by Hall et al. (1996) and depicted in the Figure 9. The phases selected for extraction are categorized into five steps:

- **Fraction I** – adsorbed/exchangeable/carbonate:
- **Fraction II** – amorphous Fe oxyhydroxide (AEC):
- **Fraction III** – crystalline Fe oxide;
- **Fraction IV** – sulphides and organics;
- **Fraction V** – residual, mainly silicates.

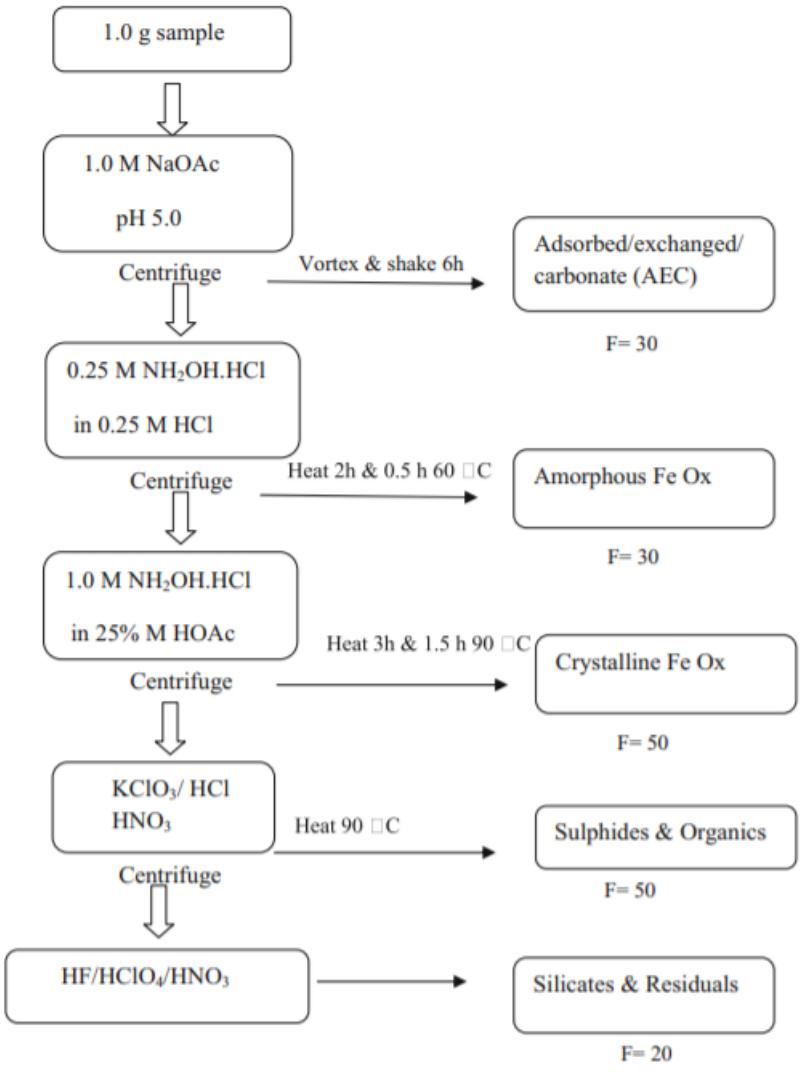

Figure 9 *– REE sequential extraction procedure for sediments (Hall et al. 1996).*

The order of mobility of the REEs can be calculated considering their relative abundance in each of the 5 above mentioned fractions. The order is the following: adsorbed/exchangeable/ carbonates (Fraction I) > bound to silicates and residual oxides (Fraction V) > bound to sulphides and organics (Fraction VI) > bound to amorphous Fe oxyhydroxides (Fraction II) > bound to crystalline Fe oxyhydroxides (Fraction III). Consequently, the average potential mobility of REEs can be arranged

in decreasing order as follows: Yb>**Gd**>Y=Dy>Pr>Er>Tm>Eu>Nd>Tb>Sc>Lu>Ce>La. There are many factors that control the mobility of REEs in the aquatic ecosystem. Such factors may include pH, climatic conditions, weathering and nature of rocks, dissolution, solubility, ionic radius, dissolved ionic species, alluvial deposits and adsorption capacity (Khan et al., 2016). However, it must be mentioned that, due to the low concentration of REEs and due to the high concentration of the interfering matrix components, determination of REEs in environmental samples is not an easy task. In fact, samples usually require a pre-concentration and separation step. An alternative method for REEs separation is the solid phase extraction (SPE) (Pyrzynska et al., 2016). In this technique, REEs are sorbed on different water-insoluble solid materials and further eluted with acids or complexing reagents. Solid phase extraction procedures offer several important advantages in comparison with classical liquid-liquid extraction, such as reduced organic solvents usage and exposure, high enrichment factor, rapid phase separation and the possibility of combination with different detection techniques (Augusto et al., 2013). Several nanomaterials can be employed as solid phase sorbents such as carbon nanotubes, graphene oxide and molecularly imprinted nanoparticles (Pyrzynska et al., 2016).

2.3.2 Speciation of gadolinium in water and sediment samples worldwide

The number of studies regarding Gd speciation in water and sediment samples is quite low, and further quantitative speciation studies are urgently needed to understand the fate of the contrast agents in the environment, especially the uptake into biological systems. In this scenario, Lindner et al. (2013) analysed surface water samples from the Teltow channel, near Berlin (Germany) in order to determine Gd speciation employing the HILIC, coupled with inductively coupled plasma mass spectrometry (ICP-MS) method. Using these two techniques, two different Gd-containing contrast agents have been detected: Dotarem (Gd-DOTA) and Gadovist (Gd-BT-DO3A). The same authors also reported that other contrast agents such as Gd-BOPTA and Gd-DTPA have been detected in other locations in the area of Berlin, demonstrating their wide employment in the country. The concentration of Gd-DOTA and Gd-BT-DO3A in the WWTP water outlet was approximately 456 and 471 ng/L, respectively, way far above the geogenic background (Lindner et al., 2013). Further downstream, the concentration of both forms decreased to about 65 ng/L. These data confirm that there was no significant degradation or decomplexation of the gadolinium-based contrast agents over a distance of the first 5 km after the inlet of the wastewater into the Teltow channel, because no additional peaks or shifts in retention time have been observed in chromatograms (Lindner et al., 2013). In addition, Altomare et al. (2020) reported noteworthy Gd anomalies in the Orlando

Easterly Wetlands (OEW) sediments, detecting an average ratio Gd_{Ant}/Gd_{Geo} of 5.34. One of the meaning of this result can be found in previous studies (Verplanck et al., 2005) on aqueous Gd^{3+} speciation which have shown that the metal ion forms tends to complexate with carbonate and phosphate if present in high concentrations. About this latter topic, precipitation of REEs with phosphate has been reported as a possible mechanism for inorganic sedimentation of gadolinium (Byrne et al., 1996). Thus, the amount of phosphorus entering the OEW may provide opportunity for Gd–P precipitation and/or complexation reactions, even if no correlation between phosphorus and Gd has been found in the present article (Altomare et al., 2020). In addition, differences in Gd concentration in sediments have been noted according to the changes in sediment composition (Altomare et al., 2020). In fact, in samples containing high amounts of sandy material, a lower amount of anthropogenic Gd has been noted. On the other hand, samples with greater quantities of total organic carbon (TOC), had higher concentrations of Gd_{Ant}, suggesting that Gd sequestration may occur through uptake by plants and/or through deposition of natural organic matter (Altomare et al., 2020).

Researches showed that not only medical facilities are responsible for Gd pollution. In fact, Khan et al. (2016) reported that also mining activities release REEs into natural water both via the direct discharge of wastewaters that contain high levels of these pollutants and through the leaching process of sediments enriched in REEs. When REEs enter the aquatic environment, they are distributed between aqueous and suspended sediments. REEs in sediments could assimilate with organic matters, Fe oxides, sulphides, and clay, since sediments are potential reservoirs for trace metals. A speciation analysis of sediments in ex-mining lakes in Malaysia allowed to determine the percentage of Gd metal in each sediment fraction (Khan et al., 2016). 41.8 % of Gd was present in Fraction I (adsorbed/exchangeable/carbonate) and 11.0 % in Fraction II (amorphous Fe oxyhydroxide fraction), which is higher than other REEs such as La, Y and Ce, tested using the same conditions. It is noteworthy that oxides exist as nodules and cement between particles. These oxides hold the REEs and can be mobilized via reduction and acidic condition (Khan et al., 2016).

Moreover, analysis of anthropogenic Gd compounds and the assessment of their stability in water mediums is also of paramount importance. On this topic, Birka et al. (2016a) carried out a specific analysis of water samples from several waterworks in a densely populated region of Germany alongside the river Ruhr. In addition, drinking water samples have been investigated in the same research, in order to determine the possible effect of drinking water purification on these highly polar microcontaminants. For this purpose, HILIC and inductively coupled plasma-mass

spectrometry (ICP-MS) have been employed. Analysis of chromatograms showed the presence of the contrast agents Gd-BT-DO3A, Gd-DOTA and Gd-DTPA in samples from different steps of the drinking water purification, while Gd-BOPTA was not detectable in any sample (Birka et al., 2016a). Therefore, Birka et al. (2016a) results enlightened that different contrast agents can be detected and quantified in the surface water after all purification steps, and in the disinfected drinking water. Moreover, in Table 4 the Gd-based contrast agents concentration ranges have been reported, detected through the water sample analysis in different zones along the Rhur river.

Table 4. Gadolinium-based contrast agents concentration ranges expressed in pmol/L found in different sampling points along the Rhur river, Germany. Concentrations have been determined by means of HILIC-ICP-MS and total gadolinium was determined by means of ICP-MS (modified from Birka et al. 2016a).

Sample	Gd-based contrast agents				Total Gd[a]
	Gd-BT-DO3A	**Gd-DOTA**	**Gd-DTPA**	**Sum[a]**	
Waterwork A					
Surface water	<LOQ[a]	55 (±20)	161 (±1)	216	307 (±4)
After filtration	<LOQ[a]	49 (±15)	167 (±8)	216	273 (±5)
Drinking water	/	<LOQ	159 (±8)	159	254 (±3)
Waterwork B					
Surface water	<LOQ[a]	<LOQ	88 (±1)	88	161 (±1)
Ground filtration	<LOQ[a]	<LOQ	89 (±5)	89	161 (±1)
Drinking water after disinfection (UV irradiation)	/	/	82 (±22)	82	161 (±1)
Waterwork C					
Surface water	40 (±3)	<LOQ	93 (±6)	133	133 (±1)
Ground filtrate	30 (±4)	<LOQ	121 (±20)	151	130 (±1)
Drinking water after disinfection (chlorine dioxide)	<LOQ	/	94 (±13)	94	123 (±2)
Waterwork D					
Surface water	30 (±5)	56 (±20)	116 (±4)	202	231 (±5)
Ground filtrate	<LOQ	48 (±9)	128 (±22)	176	227 (±4)
Drinking water after disinfection (UV irradiation)	<LOQ	45 (±4)	110 (±27)	155	188 (±3)
Waterwork E					
Surface water	49 (±14)	61 (±2)	100 (±9)	210	242 (±6)
Ground filtrate	26 (±6)	81 (±5)	137 (±42)	244	274 (±7)

Drinking water after disinfection (chlorine dioxide)	<LOQ	74 (±24)	122 (±10)	196	298 (±1)
Waterwork F					
Surface water	38 (±20)	85 (±12)	139 (±8)	262	265 (±9)
Ground filtrate	<LOQ	37 (±18)	124 (±25)	161	218 (±4)
Drinking water after disinfection (chlorine dioxide)	<LOQ	44 (±3)	103 (±20)	147	216 (±5)

[a]The comparison of summed up concentrations of individual contrast agents and the total Gd concentrations in the surface water and drinking water samples shows a gap in the mass balance. This gap is increased in the drinking water mostly due to the extremely low concentrations of Gd-BT-DO3A, which is found below the LOQ in most samples.

As it can be noted from Table 4, waterworks D, located in more densely populated region, showed an increasing in the total Gd concentration as well as higher concentrations of individual species in the surface water, showing the presence of a significant anthropogenic input. The analysis of the samples from waterworks E also showed high concentrations of total Gd and contrast agents compared to the waterworks B and C upstream the Ruhr river. In addition, the analysis of samples from the waterworks E and F, indicates an increased anthropogenic input of Gd downstream the Ruhr river. The concentrations of contrast agents were also clearly increased in the drinking water produced from the related waterworks (Birka et al., 2016a). These results evidence not only the presence of anthropogenic Gd-MRI contrast agents in German rivers, but also that these pollutants are not degraded by conventional purification methodologies, remaining almost unaltered in the drinking water (Birka et al., 2016a).

These data are in accordance with those obtained in another paper published by Birka et al. (2016b) in which solutions of four widely applied contrast agents have been irradiated with UV light and successively analysed by means of HILIC-ICP-MS. These experiments aimed to test the stability of possible Gd-contrast agents transformation products, with particular attention on the release of Gd(III) ions resulting from transmetallation reactions. The results showed that the concentration of Gd-DTPA, Gd-DOTA and Gd-BT-DO3A did not decrease after 300 min of irradiation, while there is a significant decline of the amount of Gd-BOPTA to 85%. This latter fact can be explained considering that Gd-BOPTA possesses an aromatic system, which is known to be less stable towards UV radiation. A further experiment investigated the photochemical degradation of Gd-BOPTA with a maximum irradiation time of 300 min in different matrices: purified water, unfiltered surface water, filtered surface water and drinking water (Birka et al. 2016b). The result obtained showed a significant decrease of the Gd-BOPTA signal, as well as the formation of several transformation products with increasing irradiation time. Due to the isocratic HILIC employed, the decrease of the

signal of Gd-BOPTA can be considered as directly proportional to the increasing signal of the transformation products. In addition, it is worth noting that the majority of transformation products elutes after Gd-BOPTA, indicating a higher polarity than the original contrast agent. By means of HILIC-ICP-MS, it was possible to demonstrate the matrix-dependent degradation of Gd-BOPTA. Additionally, HILIC-ESI-MS measurements were conducted to obtain structural information on the degradation products (Figure 10) (Birka et al., 2016b).

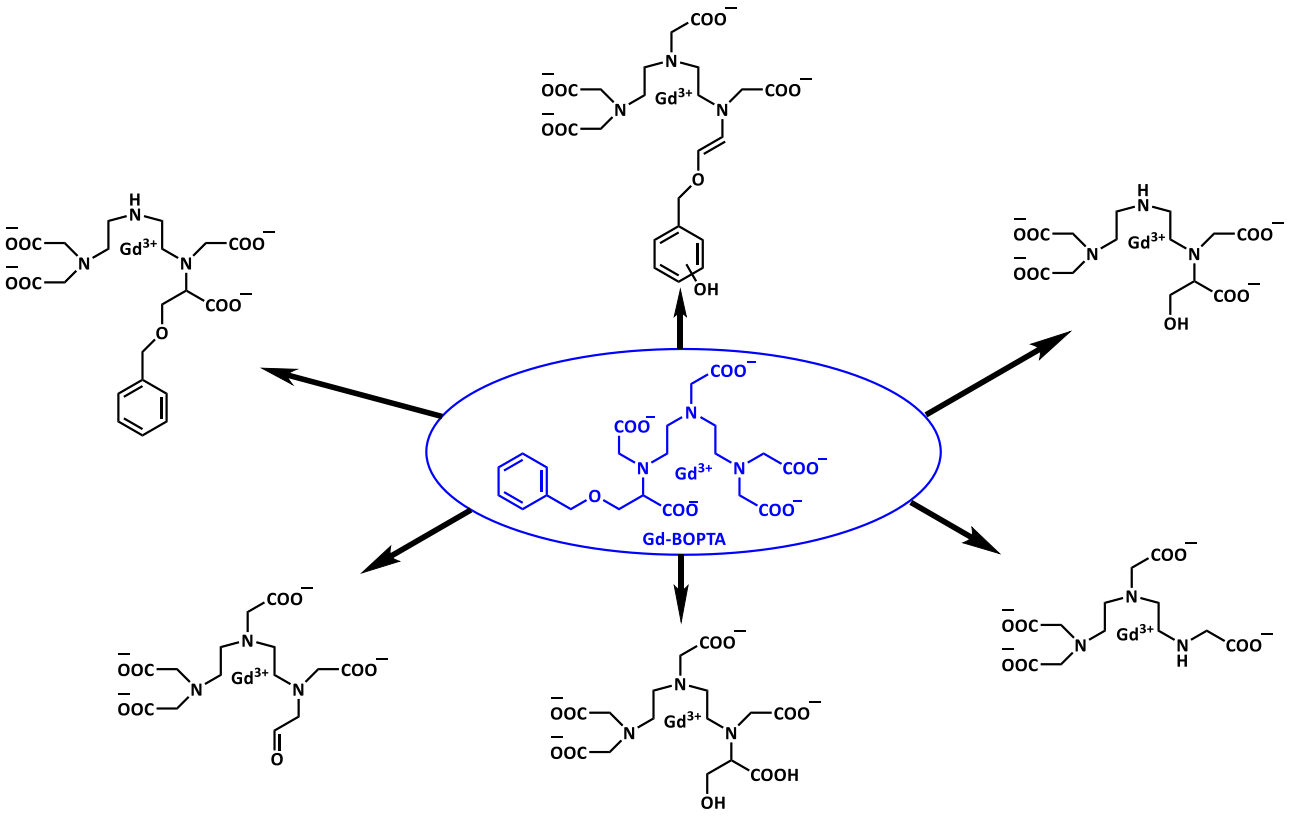

Figure 10 *– Possible Gd-BOPTA UV degradation compounds*

3. Gadolinium bioaccumulation in aquatic organisms

Articles in the literature concerning REEs showed that even aquatic organisms are able to uptake REEs from water solutions (Cyris, 2013; Rogowska et al., 2018; Freitas et al., 2020a, 2020b; Mestre et al., 2019; Pinto et al., 2019) and from sediments (Pastorino et al., 2020). Like other chemical elements, Gd toxicity is influenced by the characteristics of the organisms exposed such as age, size, the form of exposure (chronic – for a long period of time; or acute – for a short period of time) and the concentrations of other REEs in solution. Researches have shown that dose-response relationship of these metals are generally biphasic, with stimulatory or beneficial effects at low concentrations, and inhibitory or toxic effects at high concentrations (Pagano et al., 2015). Several

studies have shown that low REE quantities promote growth of both terrestrial and aquatic organisms, some of which have been used since 1990 as micronutrients in fertilizers and more recently as livestock feed additives (He and Rambeck, 2000; Xun et al., 2014). Gadolinium and in general all REEs toxicity studies have focused particularly on species of economic interest or those related directly to public health, such as the bacteria *Vibrio fischeri* (Gonzalez et al., 2015), the plants *Raphidocelis subcapitata* and those belonging to *Chlorella sp*ecies (Hao et al., 1997; Fujiwara et al., 2008; Balusamy et al., 2015; Gonzalez et al., 2015; Joonas et al., 2017). Nevertheless, researches involving more marine and freshwater species have been reported recently, thus covering a greater biodiversity (Blaise et al., 2018; Pinto et al., 2019; Duarte and Caçador, 2020; Freitas et al., 2020a, 2020b; Moreira et al., 2020).

In the next sections, Gd concentrations in different aquatic species will be discussed, including measurements in animals from the field and from laboratory exposures.

3.1 Gadolinium bioaccumulation: environmental measurements

3.1.1 Gadolinium bioaccumulation in *Pecten maximus*

Based on the discoveries done by Hanana et al. (2017), which stated that Gd exposure affects mitochondrial and anti-inflammatory pathways in freshwater mussels (see section 3.4.2), other studies tried to determine the Gd impact on other invertebrate species. In particular, Le Goff et al. (2019) studied REEs accumulation in great scallop (*Pecten maximus*). In addition, a comparison between shell samples collected from different mussel species in different worldwide coastal areas have been performed. On this topic, pronounced Gd anomalies in mollusc shells' chemical composition have been noted all around the word, making of this metal an increasing threat for marine organisms. Moreover, data analysis enlightened that the shapes of REEs patterns were similar to those of other coastal shellfish, suggesting that Gd could be uptake by a wide variety of molluscs, regardless of their species (Le Goff et al., 2019).

It must be mentioned that in bivalves, shell composition is derived from organic matter, inorganic particles and water that have been assimilated by the molluscs. For this reason, elemental composition of the annual incremental laminations that compose the shells of these organisms can reflect the elemental levels present in the aquatic medium at the time of shell construction (Markich et al., 2002). In particular, *P. maximus* have been found to display small but significant positive Gd anomalies, which indicate that shells incorporated small amounts of anthropogenic Gd. These

excesses in scallop shells (ΔGd = 0–2.3 ng/g) have been found to display a complex temporal evolution.

The oldest sample collected in 1960[7], before the use of GBCAs, did not show any significant excess in Gd. Instead, a marked increase in Gd excesses has been observed from 1989 to 2005, followed by a sharp decline until 2010 when normal levels have been observed again (Le Goff et al., 2019). Afterwards, the excesses seem to increase again without reaching the 2005 maximum. Such an evolution is unexpected because the use of GBCAs has always been increasing since their introduction on the market. In fact, GBCAs had an exceptional safety reputation from 1988 to 2006, to the point that in 2004 and 2005 these compounds were recommended as a substitute for iodine-based contrast media in patients with renal failure for CT (computed tomography) and in interventional studies (Ramalho et al., 2016). However, this trend could be explained considering the bioavailability of anthropogenic gadolinium as determined by its speciation in seawater (see section 2.3). In fact, over the last thirty years, various GBCAs have been used and their behaviours in seawater could be very different. Le Goff et al. (2019) focused their analysis on those GBCAs which were majorly used prior to 2007 in France: gadoterate meglumine (Gd-DOTA - Dotarem), gadopentetate dimeglumine and gadodiamide (Gd-DTPA – Magnevist and – Omniscan respectively) which have been depicted in the figure below (Figure 11).

[7] *Medic'AM database (2018) maintained by the Sécurité Sociale, available from, https://ameli.fr/l-assurance-maladie/statistiques-etpublications/donnees-statistiques/medicament/medic-am/medic-am-mensuel-2018.php.*

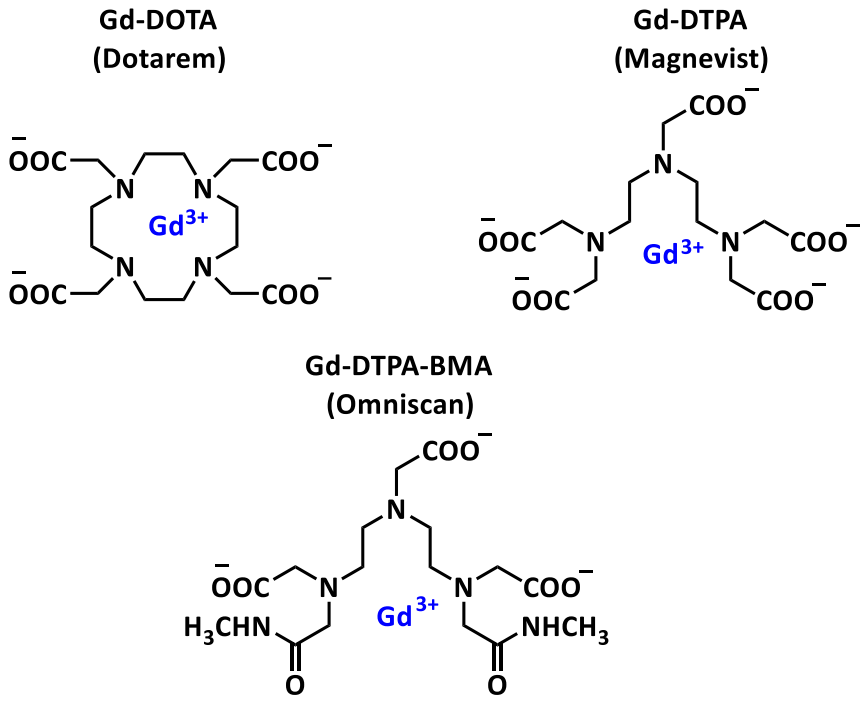

Figure 11 *– Chemical structures of Gadolinium-based contrast agents (GBCs) commonly used prior to 2007 in France (Le Goff et al., 2019).*

When the link between nephrogenic systemic fibrosis and the administration of linear GBCAs was suspected around 2005, the prescriptions of some of them were considerably reduced, notably the gadopentetate dimeglumine (Grobner, 2005; Marckmann, 2006). As a consequence, a sudden reduction of the Gd excesses in the shells has been reported, which is consistent with the abandonment of this agent. Today, Gd consumption by MRI in France is three times higher than of 2005, but the magnitude of this increase is not recorded by scallop shells. This could suggest that the bioavailability of anthropogenic Gd currently present in coastal areas is low (Le Goff et al., 2019). One of the main reasons of GBCAs low bioavailability can be attributed to their high stability in fresh water. In fact, as seen in previous sections of this thesis, anthropogenic Gd seems not to be very reactive and can be used as a useful tracer of the effluents of water-waste treatment plants (Kulaksız and Bau, 2007). Even if accumulations of Gd have been detected in digestive glands and gills of a few fresh water bivalves (Perrat et al., 2017) their shells do not show noticeable positive Gd anomalies, suggesting that the GBCA molecules have been degraded little or not at all by these molluscs (Le Goff et al., 2019).

On the other hand, little is known about the stability of GBCAs in marine waters, with only few studies regarding gadopentetate dimeglumine. Schijf et al. (2018) reported that this contrast agent

is substantially dissociated upon mixing of river water with seawater in estuaries (Schijf and Christy, 2018). Once these molecules are degraded, the Gd associated with them can become bioavailable and possibly toxic. This could explain the incorporation of anthropogenic Gd by scallop shells seen until 2005–2006. The lack of a clear correlation between the Gd excesses recorded by the shells and the consumption of the other GBCAs from 2010 to today could suggest that the latter, particularly the most used macrocyclic GBCAs, are extremely stable in seawater. However, although the use of linear GBCAs is now marginal in France (10% of gadolinium used in MRI was in the form of linear GBCAs in 2017), Gd excesses are still measured in shellfish.

3.1.2 Gadolinium bioaccumulation in Dreissena rostriformis bugensis and Corbicula fluminea organisms

As part of the article reported in the section 3.2.2, Perrat et al. (2017) studied the effects of gadolinium in two freshwater bivalve species, namely *Dreissena rostriformis bugensis* and *Corbicula fluminea* through an i*n-situ* experiment (exposition in the environment). For this purpose, Gd concentration has been determined in organisms' tissues after exposing them for 7 and 21 days in 4 different locations in the Mosel River, France, close to WWTP of Metz city. Also water samples were collected and they displayed the presence of anthropogenic Gd, whose concentration was estimated to be varying from 40 to 630 ng/L thanks to the following statistical model (Perrat et al., 2017). Gadolinium concentrations measured by ICP-MS were normalized (GdN, SmN, TbN) using the Upper Continental Crust (UCC) table, which is the most realistic table concerning aquatic environments in the Lorraine region. Then, the Gd anomaly (Gd*) was estimated using the following equation (Taylor and McLennan, 1985):

$$Gd^* = Gd_N/(Sm_N * 0.33 + Tb_N * 0.67)$$

If Gd* is found to be superior to an anomaly threshold (determined considering a reference site concentration), the anthropogenic (Gd_{anth}) and geogenic (Gd_{geo}) part of Gd can be obtained by the following calculation:

$$Gd_{anth} = Gd_{mes} - Gd_{geo} = Gd_{mes} - (\frac{Gd_{mes}}{Gd^*})$$

With Gd_{mes} as the measured concentration of Gd in the water sample collected.

The results of Gd bioaccumulation in bivalves have been also assessed, differentiating samples taken upstream and downstream the WWTP. In the whole organism, for both *D. rostriformis bugensis* and *C. fluminea*, no significant difference was observed between the upstream and the downstream locations after 21 days of exposure. This observation suggested that the WWTP effluents had no

impact on the bioaccumulation of gadolinium in bivalves in these experimental conditions, further evidencing that WWTPs are not able to retain these toxic compounds, which are instead released in the environment (Raju et al., 2010; Perrat et al., 2017).

Considering the bioaccumulation in the gills, the values were close to zero after 7 and 21 days of exposure for *C. fluminea* and a time-dependent accumulation was observed for *D. rostriformis bugensis*. Considering the bioaccumulation in the digestive gland, this time dependence was only partially observed. The concentrations of gadolinium after 21 days of exposure were higher for *D. rostriformis bugensis*. The differences between the two bivalve species could be explained by a higher activity of the defence mechanisms in *C. fluminea*, especially in the gills (Perrat et al., 2017). It is possible to assume that the defence is mainly performed by multixenobiotic resistance mechanisms as previously described (Achard, 2004). This type of mechanisms could expel out of the gills both Gd ions as well as other Gd speciations, which could be chelated to organic compounds or particles. Up to now, in literature, no specific pathways for the exclusion of free Gd and other REE have been described. Data concerning bioaccumulation of Gd for both organisms have been depicted in the following table (Table 5).

Table 5. *In situ* measurement of Gd concentrations expressed in nanograms of Gd per g of dry weight tissue for the digestive gland (DG) and the pair of gills (G) after exposure of each bivalve species (modified from Perrat et al. 2017).

	Dreissena rostriformis burgensis				*Corbicula fluminea*			
	DG[a]		**G[a]**		**DG[a]**		**G[a]**	
	7 days	21 days	7 days	21 days	7 days	21 days	7 days	21 days
In situ	75± 15	100± 18	11± 9	123± 34	6± 0	57± 24	0± 0	8± 7

[a]Concentrations expressed in ng/g_{DW}

As depicted in Table 5, Gd accumulation in bivalve tissues occurs either when organisms are exposed to a mixed solution of Gd (geogenic and anthropogenic during *in-situ* experiment) and to only one gadolinium speciation (Gd-DOTA during laboratory experiment; see section 3.2.2) (Perrat et al., 2017). However, even if the *in-situ* Gd water concentrations were much lower (40 - 630 ng/L) compared to the one present in the laboratory experiment (1, 10 µg/L), an overall greater bioaccumulation of this pollutant in the former case has been reported. This fact could majorly be due to the different Gd speciation. In fact, as reported by other literature articles (Hanana et al., 2017; Le Goff et al., 2019), chelated GBCAs, are less bioavailable compared to free Gd ions. In addition, it must be pointed out that, due to the technical approach used in this study (measurement

of Gd concentrations by ICP-MS analysis) it has not been possible to distinguish the anthropogenic Gd from the geogenic one present in bivalves' tissues during the *in-situ* experiment.

In accordance to the researches of Perrat et al. (2017), successive *in-situ* studies performed by Pereto et al. (2020), reported Gd bioaccumulation in *C. fluminea* soft tissues in the Jelle River (Bordeaux area, France), near a WWTP effluent, with a total Gd concentration ranging from 49 ± 4 and 110 ± 19 ng/g_{DW}. Anthropogenic Gd concentration instead has been estimated to be between 1.5 ± 1 and 4.1 ± 0.7 ng/g_{DW}. Despite the lower bioavailability and concentration in river waters of Gd_{anth} compared to Gd_{geo}, a clear accumulation of this contaminant in *C. fluminea* has been observed. For this reason, this organism appears to be an appropriate model species for *in-situ* monitoring of REE contaminations such as medical origin Gd (Pereto et al., 2020).

3.1.3 Gadolinium bioaccumulation in Corbicula fluminea shells

As reported in paragraph 3.1.1, bivalves are able to accumulate organic matter and inorganic particles in their shells. In particular, Le Goff et al. (2019) determined that Gd can be accumulated as well following an analogous procedure. Thus, analysis of the shell composition can be used to determine the presence also of anthropogenic REEs in water environments (Le Goff et al., 2019). On this topic, Merschel and Bau (2015) reported an unusual Gd accumulation in *C. fluminea* shells collected in the Rhine river, Germany. REEs concentrations in *Corbicula* shells covered a wide range, which strongly suggests that metal availability in the habitat was not the only factor contributing to the variability of the data. In fact, Weltje et al. (2002) and Graney et al. (1984) found that Cd uptake of *C. fluminea* is dependent on pH, temperature and substrate. Thus, a similar behaviour is expected also for Gd. REEs concentrations in organisms' shells have been reported in Table 6.

Table 6. REEs concentrations in ng/kg in river water of selected sites from the Rhine and Weser River. REE concentrations in *Corbicula fluminea* in µg/kg for different locations at the Rhine and Weser Rivers. Data have been adapted from Kulaksiz and Bau (2013, 2007) and Kulaksiz (2012).

	REEs in water samples (ng/Kg)		**REEs in *C. fluminea* shells (µg/Kg)**	
	Rhine River	Weser River	Rhine River	Weser River
La	31.88[a]	10.5	493.16[a]	64.7
Sm	3.90[a]	3.26	8.55[a]	12.1
Gd	11.54[a]	19.4	6.82[a]	11.6

[a]data averaged from REEs concentrations measured in different locations of the Rhine river, Germany.

From the analysis performed, it has been determined that, in spite of the omnipresence of anthropogenic positive Gd anomalies in Rhine River and Weser River waters, a similar anomaly was not shown by the *Corbicula* shells. In fact, while anthropogenic La and Sm from an industrial point source to Rhine River water were readily incorporated into the shell, the anthropogenic Gd from diffuse sources (MRI contrast agents present in the discharge from WWTPs into the Rhine and Weser rivers) was not. The incorporation of anthropogenic La and Sm into the *Corbicula* shells suggests that these REE micropollutants are bioavailable. Moreover, considering that they have also been detected in tap water used as drinking water along the Rhine River, further studies on their potential ecotoxicological effects are required. On the other hand, the discrimination against incorporation of anthropogenic Gd corroborates previous evidence of the long environmental half-life of the Gd-compounds used as contrast agents (Laurent et al., 2006). These data contribute also in evidencing once again that the conservative behaviour of anthropogenic Gd makes it a useful tracer of WWTP effluents in river, lake, ground and tap waters (Merschel and Bau, 2015).

3.2 Gadolinium bioaccumulation: laboratory exposures

3.2.1. Gadolinium bioaccumulation in Mytillus galloprovincialis

Henriques et al. (2019) determined Gd concentration in *Mytillus galloprovincialis*' soft tissues after a chronic exposure period of 28 days. Results are reported in Table 7.

Table 7. Gadolinium (Gd) concentrations (µg/g) in mussels' soft tissues after 28 days of exposure to seawater spiked with 15, 30, 60 and 120 µg/L of Gd_2O_3. Limit of quantification (LOQ) was 0.38 µg/g dry weight (modified from Henriques et al. 2019).

Nominal concentration (µg/L)	**Gd concentrations in *M.Galloprovincialis* ($\mu g/g_{DW}$)**	**BCFs**
<0.50 (CTL)	<0.38	/
15	<0.38	/
30	0.44± 0.10	16
60	0.81± 0.070	15
120	2.5± 0.50	23

From these data, it can be noted that in organisms exposed to the lowest pollutant concentration as well as in the control ones, Gd quantities were so low to be below the quantification limit of the inductively coupled plasma mass spectroscopy (ICP-MS) used (LOQ=0.38 µg/g). Analysis performed

in mussels exposed to higher concentrations (30, 60 and 120 µg/L) revealed the presence of the element, with contents ranging from 0.44 ± 0.10 µg/g_{DW} to 2.5 ± 0.50 µg/g_{DW}. The bioconcentration factors (BCFs), defined as the ratio between Gd concentration in mussels' tissue at the end of the exposure and its initial concentration in water, were shown to be independent from the exposure conditions. These results evidence the capacity of mussels to accumulate Gd, with a direct relationship between accumulation and exposure concentration (Henriques et al., 2019).

3.2.2 Gadolinium bioaccumulation in Dreissena rostriformis bugensis and Corbicula fluminea

Perrat et al. (2017) studied the effects of gadolinium in two freshwater bivalve species, namely *Dreissena rostriformis bugensis* and *Corbicula fluminea*. Organisms' Gd uptake was analysed using specific exposure concentrations (0, 1 and 10 µg/L) and the bioaccumulation was determined in bivalves' tissues after an exposure period of 7 and 21 days. In the experiment, Gd was only used in the form of the Gd-contrast agent (Gd-CA) gadoteric acid (Gd-DOTA - Dotarem®). Due to the high stability and to the absence of any transmetallation reactions involving gadoteric acid (Dotarem®) (Laurent et al., 2006), no other origin of Gd was possible during this experiment. After the exposure to 1 µg of Dotarem®, no bioaccumulation was observed in the gills for both *D. rostriformis bugensis* and *C. fluminea* after 7 days while very low concentrations of Gd have been measured after 21 days. On the contrary, a time-dependent bioaccumulation was observed in the digestive gland of both organisms with higher Gd values when compared to the gills tissue. These data could be explained by the fact that the defence mechanisms are more efficient in the gills, which are the first tissues in contact with the external medium due to the filtering activity (Perrat et al., 2017). When the organisms were instead exposed to 10 µg/L of Gd-DOTA, the bioaccumulation was time-dependent for both *D. rostriformis bugensis* and *C. fluminea* and the concentrations of Gd were always higher in the digestive gland when compared to the concentrations of the gills. Nevertheless, the concentrations of Gd in the digestive gland were more abundant for *D. rostriformis bugensis* when compared *C. fluminea* suggesting that the defence mechanisms in this tissue are more efficient for *C. fluminea*. Gd accumulation expressed in ng per gram of dry tissue of both organisms, have been reported in the following table (Table 8).

Table 8. Laboratory measurement of Gd concentrations expressed in nanograms of Gd per grams of dry weight tissue for the digestive gland (DG) and the pair of gills (G) after exposure of each bivalve species (modified from Perrat et al., 2017).

	Dreissena rostriformis burgensis				*Corbicula fluminea*			
	DG[a]		**G[a]**		**DG[a]**		**G[a]**	
	7 days	21 days	7 days	21 days	7 days	21 days	7 days	21 days
1 µg L^{-1}	6.0 ± 5.8	77.8± 11.8	0.0± 0.0	4.7± 6.2	6.4± 6.2	33.4± 2.6	0.0± 0.0	5.4± 4.0
10 µg L^{-1}	25.0± 4.8	203± 27.8	0.0± 0.0	28.8± 8	5.4± 6.0	100.4± 19	0.0± 0.0	57.4± 3.0

[a]Concentrations expressed in ng/g_{DW}

As can be seen in the Table 8, a slight bioaccumulation of Gd-DOTA has been reported. This fact can be easily attributed to the fact that chelated GBCAs, such as Gd-DOTA employed in this experiment, are less bioavailable compared to free Gd ions. However, even if in lower extent, bioaccumulation of gadolinium coming from gadoteric acid (Dotarem®) has been observed. For this reason, further researches must be performed to determine more accurately the bioaccumulation mechanisms of these contrast agents in various aquatic organisms.

3.2.3 Bioaccumulation of $GdCl_3$ and Omniscan in Dresissena polymorpha

Hanana et al. (2017) tested the capacity of *Dreissena polymorpha* to bioaccumulate gadolinium in 2 speciation forms: $GdCl_3$ and the Gd-contrast agent Omniscan. In this experiment, mussels have been collected in Saint-Laurence river, Quebéc, Canada and successively exposed to increasing concentrations of $GdCl_3$ and Omnsican (10, 50, 250 and 1250 µg/L) for 28 days. Measurement of Gd content in the soft tissue of mussel exposed to $GdCl_3$, showed a dose dependent significant increase in Gd concentration. Results have been reported in Table 9.

Table 9. Gd concentration in soft tissue of zebra mussel exposed to different concentrations of $GdCl_3$ and Omniscan for 28 days after depuration. Variations of bioaccumulation factors (BAF) of Gd in mussel were also reported (modified from Hanana et al., 2017).

Gd concentrations (µg/L)	**$GdCl_3$**	**Omniscan**	**$GdCl_3$**	**Omniscan**
	Gd accumulation in soft tissue mg/Kg (wet weight)		BAF (L/Kg)	
0	0.001	0	0	0
10	0.43± 0.20	0.03 ± 0.03	43	3
50	1.35 ± 0.27	0.13 ± 0.08	27	2.6

250	3.18 ± 1.16	0.14 ± 0.03	12.72	0.56
1250	44.97 ± 24.48	0.30 ± 0.08	36	0.24

Conversely to what exhibited by $GdCl_3$, exposure to Omniscan showed a lower amount of Gd detected in organisms' soft tissues for all exposure concentrations. Indeed, Gd content in mussel exposed to the highest dose of Omniscan was similar to that measured in mussel exposed to the lowest dose of $GdCl_3$ (Table 9). This finding could suggest that Omniscan does not significantly dissociate, thus avoiding the liberation of the toxic Gd^{3+} ion (Hanana et al., 2017). This is probably due to the strong complexation of Gd with the diethylenetriaminepentaacetate ligand. A similar result was previously reported in other studies which indicated that the low measured conductivity of Omniscan solution was due to the low amount of free Gd in solution (Normann et al., 1995).

3.3 Effects of metal contamination: oxidative stress and metabolism related responses

3.3.1 Oxidative stress biomarkers

Pollutants discharged in water environments usually cause an alteration of the cellular balance between prooxidant mechanisms and antioxidant defences of the target cell. In particular, studies employing marine (Pinto et al., 2019; Mestre et al., 2019) and freshwater (Perrat et al., 2017; Blinova et al., 2018) species, demonstrated that they are negatively affected by REEs, which often cause alterations on the oxidative status of the animals. These chemicals can both depress the antioxidants capacity to remove oxyradicals or enhance the intracellular formation of the so-called reactive oxygen species (ROS). Reactive oxygen species are naturally produced during several cellular pathways of aerobic metabolism including oxidative phosphorylation, electron transport chains in mitochondria and microsomes, the activity of oxidoreductase enzymes producing ROS as intermediates or final products, or even immunological reactions such as active phagocytosis (Regoli and Giuliani, 2014). The main ROS generated by cellular metabolism are the singlet oxygen $^1O_2$, the superoxide anion O_2^- , the hydrogen peroxide (H_2O_2) and the hydroxyl radical (HO•). These compounds can rapidly react to form other molecules like peroxynitrite (HOONO), hypochloric acid (HOCl), peroxyl radicals (ROO•) and alkoxyl radicals (RO•). Despite all these molecules are generally termed as ROS, they greatly differ in terms of cellular reactivity and potential to cause damage to lipids, proteins and DNA. Normally, the adverse effects of oxyradicals are prevented by the

antioxidant system, consisting of a wide array of low molecular weight scavengers and antioxidant enzymes which interact in a sophisticated network (Figure 12).

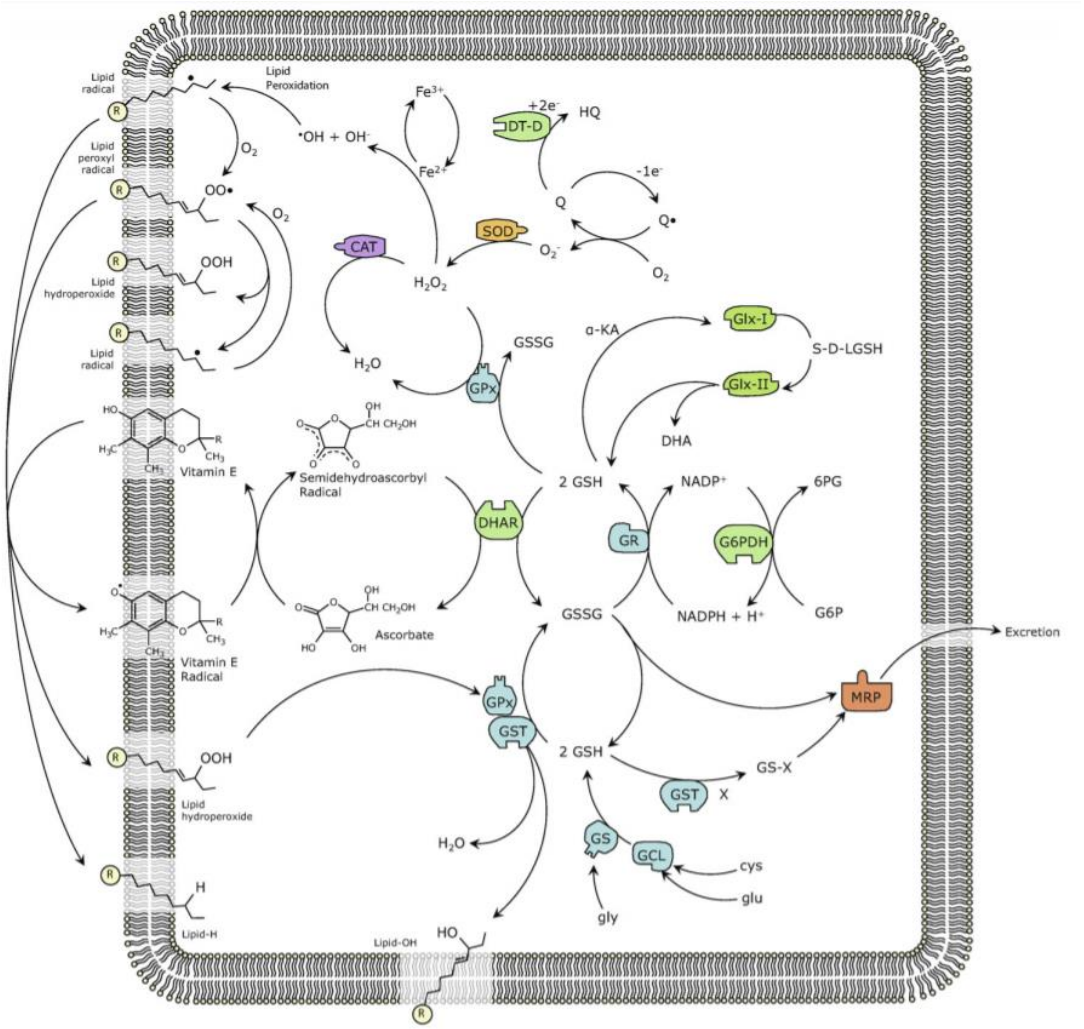

Figure 12 *-Schematic representation of the main cellular antioxidant defences and antioxidant pathways (Regoli and Giuliani, 2014).*

Scavengers neutralize ROS by direct reaction with them, thus being temporarily oxidized before being reconverted by specific reductases to the active form. Scavengers can act as antioxidants in the cytoplasm or are intended to arrest the propagation of lipid peroxidation reactions on the membranes. The most abundant cytosolic scavenger is the reduced glutathione (GSH), a tripeptide (g-glutamylecysteinyl glycine), which directly neutralizes several reactive species through its oxidation to GSSG (Regoli and Giuliani, 2014). Its red-ox equilibrium has been depicted in Scheme 2. In addition, GSH acts as a cofactor of several antioxidant glutathione-dependent enzymes (Regoli and Giuliani, 2014). Thus, under a stressful condition GSSG content is enhanced above the reducing

capacity of glutathione reductase (GRed) and the ratio GSH/GSSG is altered, decreasing along the increasing stress level. For this reason, the ratio GSH/GSSG has been frequently used as an indicator of cellular redox status after exposure to pollutants (Freitas et al., 2020a).

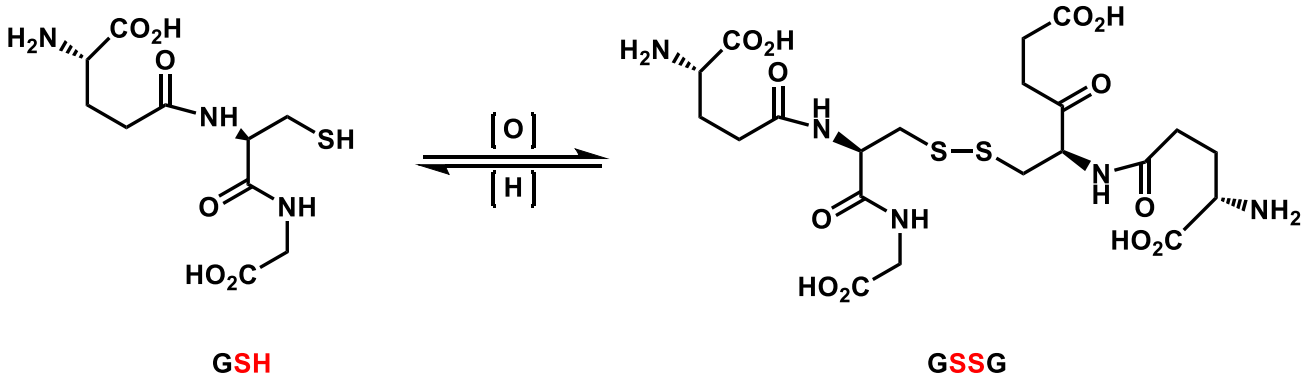

Scheme 2 *- glutathione red-ox equilibrium*

Pathways of chemically mediated ROS formation are closely related, and several indirect and cascade effects modulate both transcriptional and post-transcriptional responses of antioxidant defences. The most important mechanisms through which trace metals generate ROS depend on the ability of the former ones to lose electrons and catalyse Haber-Weiss and Fenton reactions (Scheme 3). The overall reaction generates HO• after the reduction of an oxidized metal by $O_2^{\bullet -}$ and its reaction with H_2O_2.

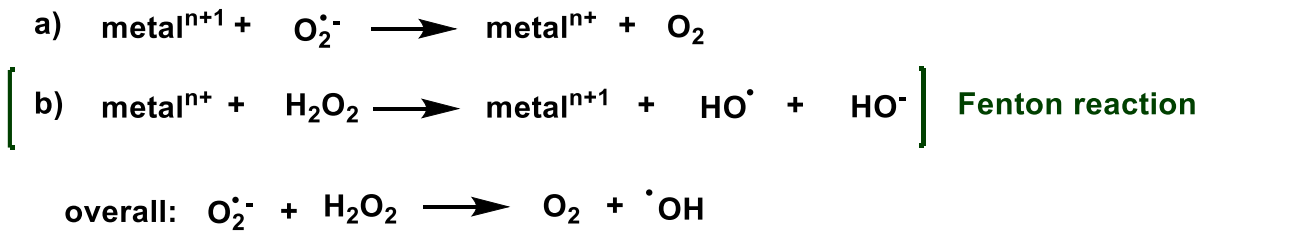

Scheme 3 *- Haber-Weiss and Fenton reactions (modified from Regoli and Giuliani, 2014).*

The Haber-Weiss and Fenton reactions are catalytically slow, unless a transition metal ion reacts with hydrogen peroxide to generate hydroxyl radical and the oxidized metal (the Fenton reaction). In addition to the reactions already showed in the previous schemes, many other prooxidant mechanisms are activated by trace metals. Among all, some can enhance intracellular generation of ROS through the activity of several oxidoreductase and flavoenzymes. This causes indirect mechanisms which involve adverse effects on mitochondrial electron transfer chain with consequent ROS release at the ubiquinone site of the respiratory chain (Regoli and Giuliani, 2014).

3.3.2 Antioxidant and biotransformation defences

Superoxide dismutase enzyme (SOD) is responsible for the removal of $O_2^{\bullet -}$ with the consequent formation of H_2O_2 (Scheme 4). This enzyme can be present in 2 forms, namely:

- SOD-Cu-Zn which is majorly present in the cytosol but also in chloroplasts and peroxisomes;
- SOD-Mn which is instead localized in the mitochondria.

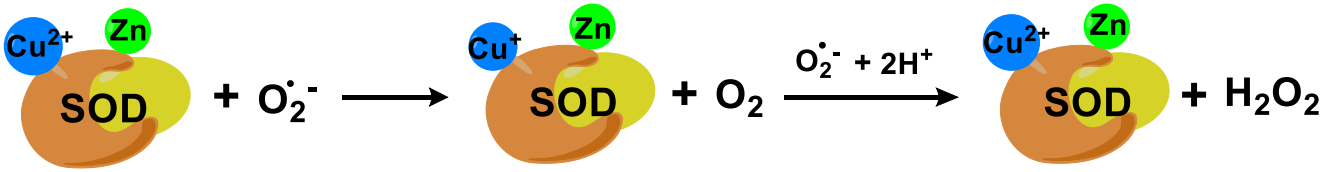

Scheme 4 *- superoxide dismutase (SOD) activity reaction.*

In order to determine the SOD activity in an organism, the method described by Beauchamp and Fridovich (1971) after adaptations performed by Carregosa et al. (2014) is usually performed. In this protocol, superoxide anions are generated starting from the conversion of xanthine and molecular oxygen in uric acid and hydrogen peroxide (H_2O_2) thanks to the action of the enzyme xanthine oxidase (XOD). The superoxide anion produced in this way, converts the tetrazolium salt NBT (nitrotetrazolium blue chloride) in a formazan dye. The addition of SOD to this reaction reduces the levels of superoxide anions, therefore lowering the formation of the dye. The enzyme activity in the experimental sample is measured as the percentage of inhibition of the rate of dye formation. This process is described in the following scheme (Scheme 5):

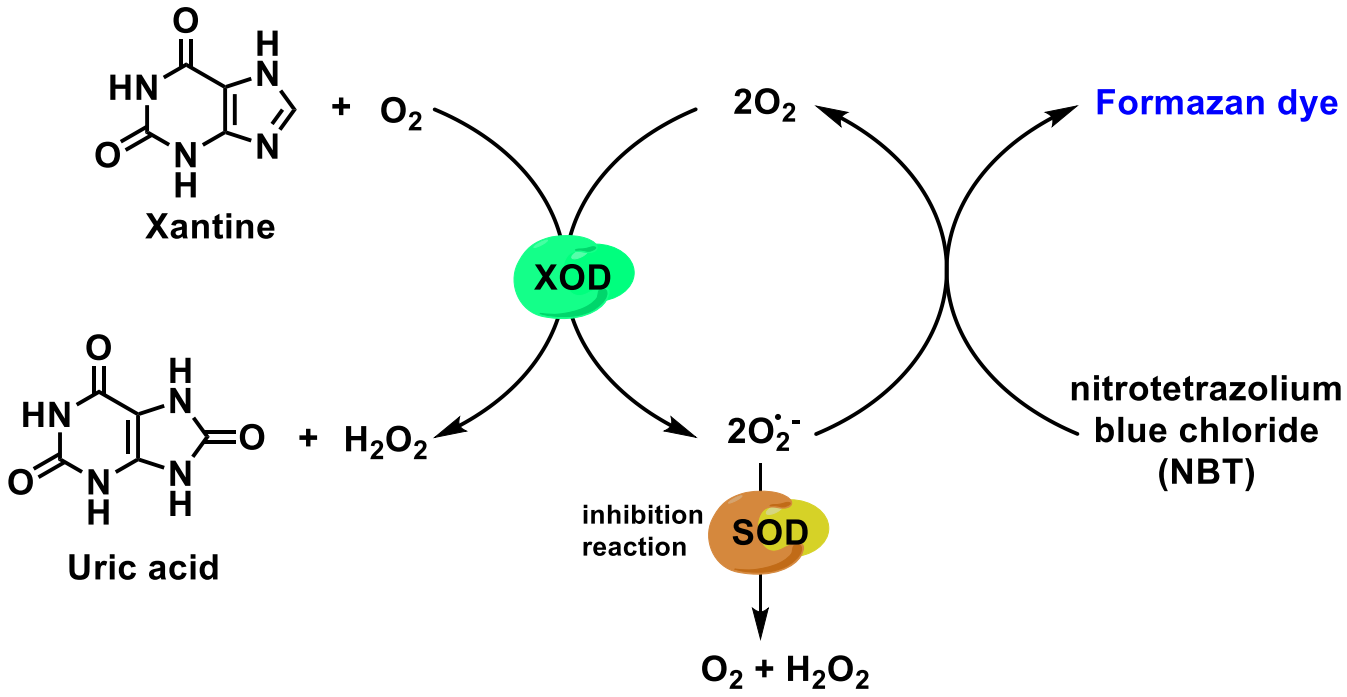

Scheme 5 *– SOD activity measurement assay using Beauchamp and Fridovich (1971) after adaptations performed by Carregosa et al. (2014).*

Finally, the determination of SOD activity is performed analysing samples' absorbance at 560 nm after 20 min of incubation at room temperature. In the end, thanks to the Lambert-Beer law, is possible to determine the concentration of the present enzyme in the sample (Regoli and Giuliani, 2014; Regoli et al., 2011).

Catalase (CAT) and glutathione peroxidase (GPx) enzymes are both involved in the reduction of H_2O_2, formed by SOD degradation of superoxide anions, into H_2O (Scheme 6). However, while the former enzyme is majorly present in both peroxisomes and cytoplasm, the latter one can be found in the cytosol and in various cellular organelles. CAT, in the presence of Fe^{2+}, converts H_2O_2 in the hydroxy radical (HO•) through the Fenton reaction. HO• is an extremely reactive initiator for the lipid peroxidation in the cellular membrane.

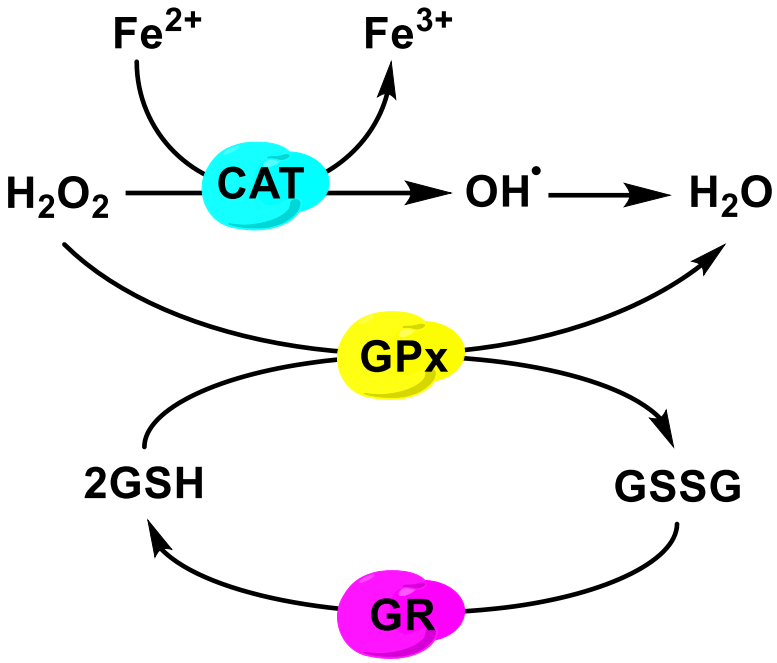

Scheme 6 *- catalase (CAT), glutathione peroxidase (GPx) and gluthatione reductase (GR) interconnected mechanism for the transformation of H_2O_2 into H_2O.*

Catalase (CAT) activity is usually quantified employing the Johansson and Borg (1988) method and the modifications performed by Carregosa et al. (2014). In this protocol, the enzyme is mixed with methanol in the presence of H_2O_2. The red-ox reaction produces formaldehyde. Afterwards, to the formaldehyde solution, the triazolic compound called Purpald is added. Potassium periodate (KIO_4) is instead used as an oxidating agent, able to catalyse the reaction between formaldehyde and Purpald, producing a purple- coloured compound and KOH as a side product. The entire process has been depicted in the following scheme (Scheme 7):

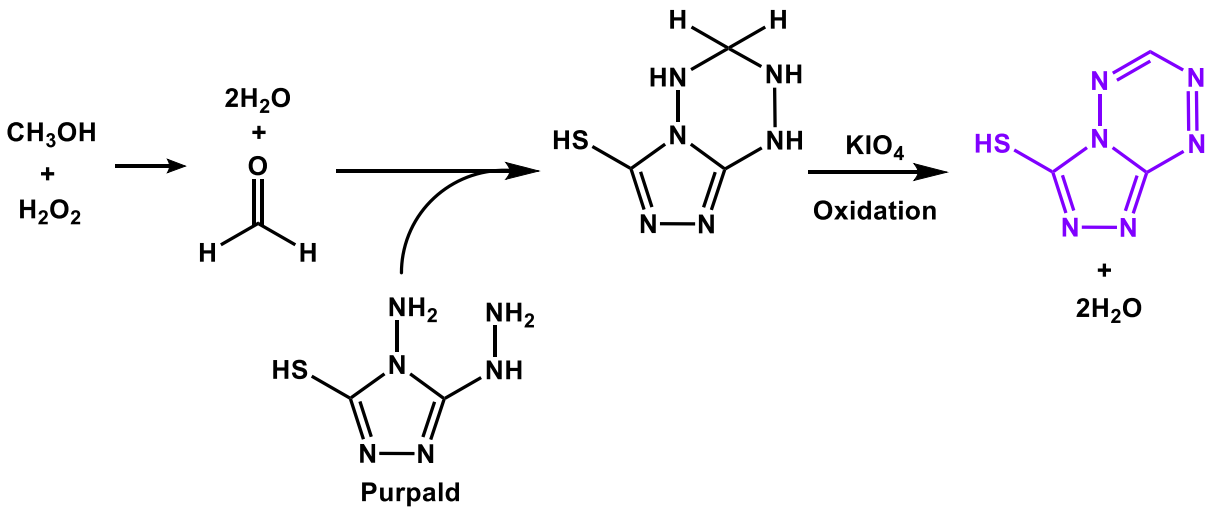

Scheme 7 *- Catalase (CAT) activity assay employing the Johansson and Borg (1988) method and the modifications performed by Carregosa et al. (2014).*

The addition of CAT enzyme to this reaction, reduces the quantity of H_2O_2 in the solution. This causes a lower amount of purple compound and consequently a lower absorbance intensity. Finally, the CAT activity is performed analysing the samples' absorbance at 540 nm. In the end, thanks to the Lambert-Beer law, is possible to determine the concentration of the present enzyme in the sample. Glutathione peroxidase (GPx) activity is instead quantified following Paglia and Valentine method (1967). GPx enzyme catalyses the cumene hydroperoxide reduction, exploiting the red-ox reaction of GSH into GSSG as a coupled process. In addition, GSSG is successively reduced to GSH thanks to the action of the glutathione reductase (GR). The cumene hydroperoxide reduction is followed by a spectrophotometer at 340 nm and the absorbance is directly proportional to the GPx concentration in the sample (Regoli and Giuliani, 2014; Regoli et al. 2011).

Glutathione S-transferase (GSTs) are a family of enzymes that catalyse the conjugation of the reduced form of glutathione (GSH) both to xenobiotic substrates and ROS for the purpose of detoxification. The reaction proceeds through the binding of GSH to compounds that contain an electrophilic centre with the consequent formation of a thioether bond between the sulphur atom of GSH and a broad range of substrates. (Scheme 8):

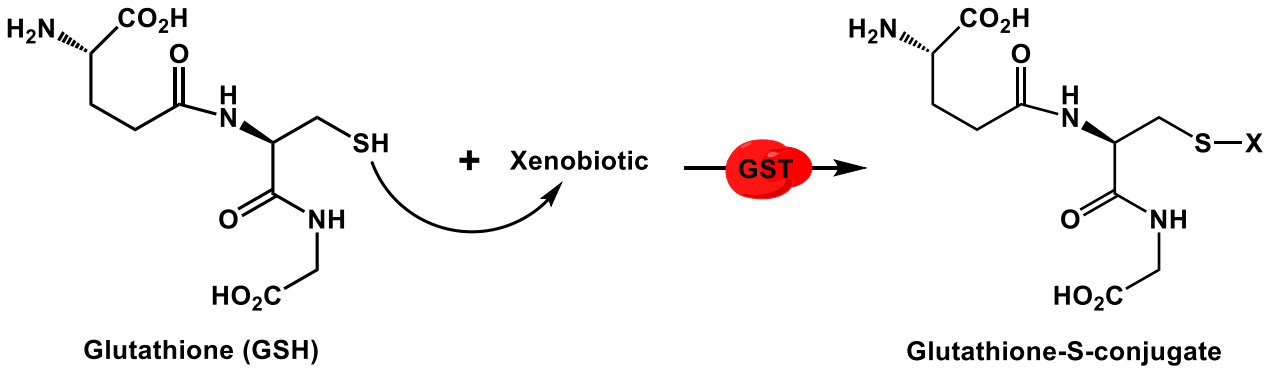

Scheme 8 *- Glutathione S-transferases reaction mechanism*

The aim of this reaction is to turn xenobiotics into more hydrophilic compounds, facilitating in this way their excretion. GSTs enzymes can also bind to toxins acting as carriers. A higher GSTs activity is often associated with a low GSH content, indicating the loss of cellular redox balance. In this way, since xenobiotics are the primary source of oxidative stress, GSTs also play an important indirect role in antioxidant defence, by eliminating toxic substances and preventing subsequent deleterious effects.

Glutathione S-transferases (GSTs) activity is usually quantified employing the Habig et al. (1974) method with some adaptations performed by Carregosa et al. (2014). In this protocol, chloro 2,4-dinitrobenzene (CDNB) is employed as a substrate. The enzyme catalyses the nucleophilic substitution of a glutathione molecule onto the CNDB with the formation of a thioether bond. The reaction mechanism is depicted in the scheme below (Scheme 9):

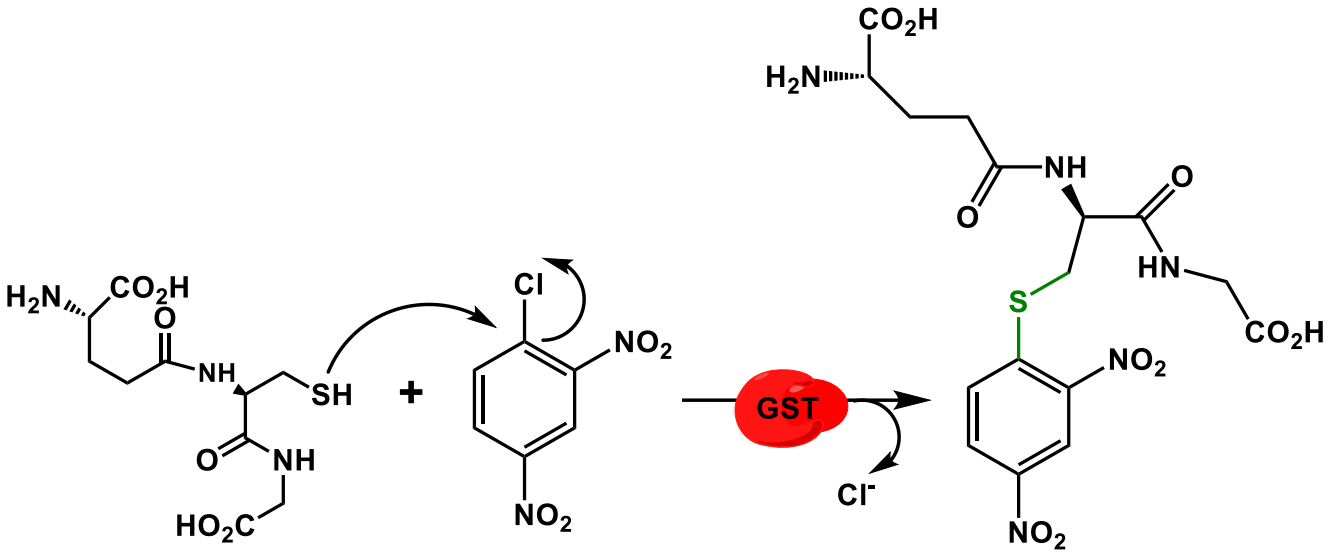

Scheme 9 *- GSTs-catalysed nucleophilic substitution reaction using chloro 2,4-dinitrobenzene (CDNB) with the formation of the final product S-(2,4-dinitrophenyl)glutathione. In the scheme is also enlightened in green the formation of a thioether bond.*

Finally, GSTs activity is measured spectrophotometrically at 340nm and thanks to the Lambert-Beer law, is possible to determine its concentration in the sample (Regoli and Giuliani, 2014; Regoli et al. 2011).

3.3.3 Cellular damage

As mentioned in the previous paragraphs, reactive oxygen species (ROS) are able to induce the peroxidation of the membrane lipids. The mechanism through which lipid peroxidation (LPO) occurs is depicted in the Scheme 10. The reaction starts with the removal of an H atom from a target lipid by means of a radical hydroxide initiator (Scheme 10, reaction A). The lipid radical formed in this way, reacts with molecular oxygen O_2, producing a peroxidised lipid radical (LOO). This reactive species immediately removes a H atom from another lipid molecule, thus propagating the reaction (Scheme 10, reaction B). Lipid peroxidation chain ends either when 2 radicals annihilate reacting together or when the radicals are destroyed by a liposoluble antioxidant.

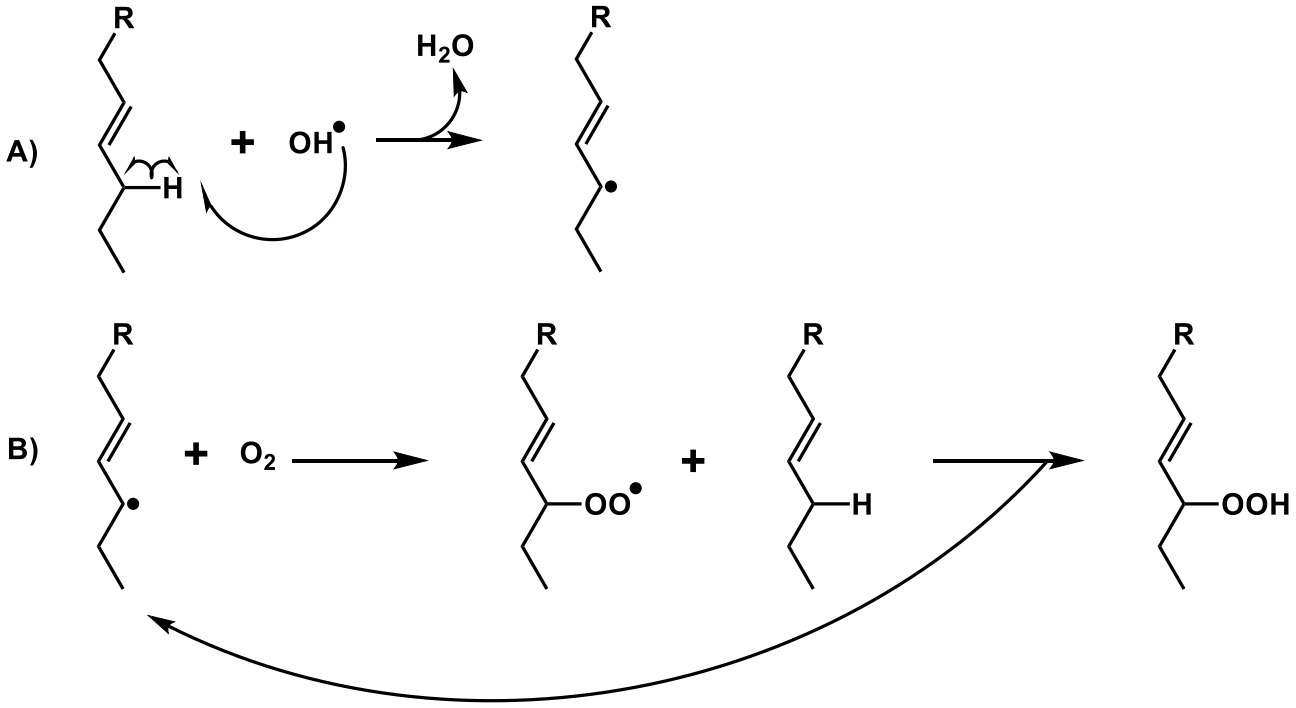

Scheme 10 *- lipid peroxidation (LPO) chain reaction mechanism. A) Initiation: the radical hydroxide reacts with a lipido molecule with the formation of a radical lipid; B) Propagation: the lipid radical formed douring the initiation process, reacts with molecular oxygen, generating a peroxidised lipid radical which immediately removes a H atom from another lipid molecule, generating a new radical and thus propagating the reaction.*

Among all the peroxidised molecules generated in the LPO process, malondialdehyde (MDA) is one of the most abundant and probably the most commonly used as an oxidative stress marker. LPO determination is performed following the method described by Ohkawa et al. (1979). In this protocol, LPO is estimated by the quantification of thiobarbituric acid-reactive-substances (TBARS), formed in the reaction between LPO by-products (such as malondialdehyde – MDA) with 2-thiobarbituric acid (TBA) (Regoli and Giuliani, 2014; Regoli et al., 2011). This reaction mechanism is depicted in the scheme below (Scheme 11):

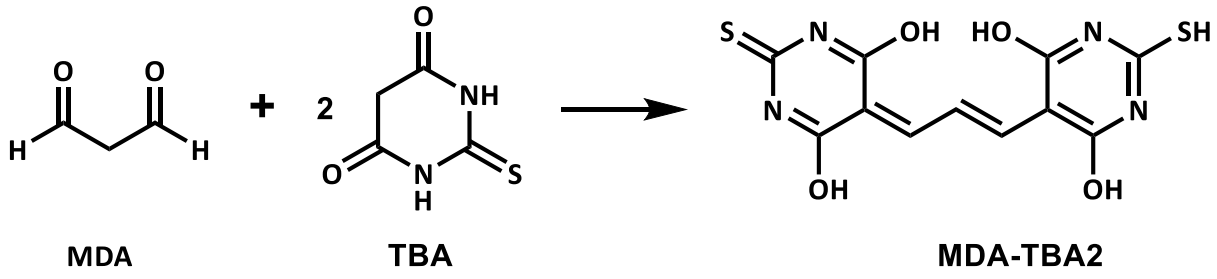

Scheme 11 *– lipid peroxidation (LPO) quantification assay using Ohkawa et al. (1979) protocol. Malondialdehyde (MDA) has been considered as the major product of lipid peroxidation.*

Protein carbonylation (PC) is also an oxidative stress biomarker, resulting from the oxidation of proteins by ROS and corresponding to the presence of carbonyl groups, such as aldehydes and ketones, in specific amino acid side chains such as lysine, proline, arginine and threonine (Freitas et al., 2020a). Typically, the carbonyl content present in proteins is determined through the Levine method (Levine et al., 1990). In this assay, carbonylated proteins are mixed with 2,4-dinitrophenylhydrazine (DNPH) in the presence of an acid as catalyser and ethanol. The product of this reaction is a chromophoric adduct, which can be analysed spectrophotometrically at 366 nm (Alomari et al., 2018). The overall reaction mechanism is depicted in the following scheme (Scheme 12).

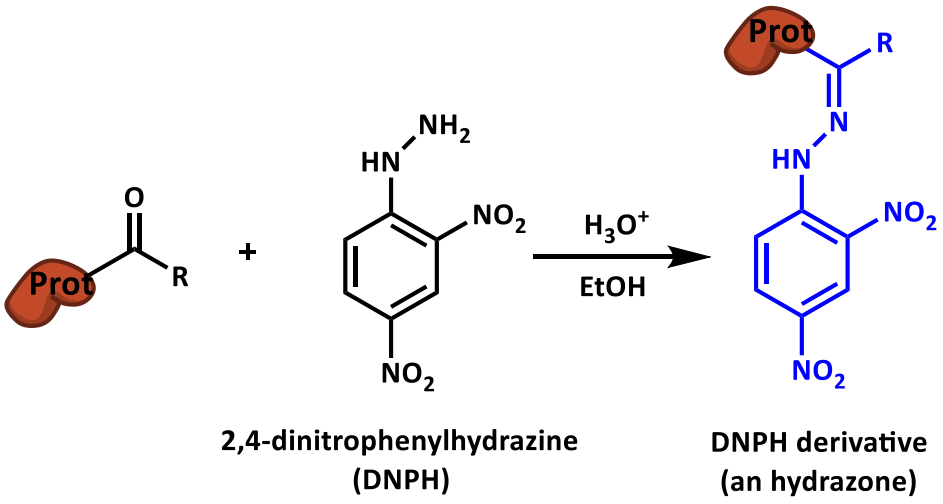

Scheme 12 *- Protein carbonylation (PC) quantification assay using Levine et al. (1990) method.*

3.3.4 Metabolism related biomarkers

In addition to the determination of oxidative stress biomarkers (section 3.3.1), having insights about the metabolic activity of the organism under study, especially after its exposure to pollutants, is of paramount importance. Cellular Energy Allocation (CEA) assay is usually employed to evaluate the effects of toxic stress on the metabolic balance of test organisms (De Coen et al., 1995). Following this approach, energy reserves available (E_a) and energy consumption (E_c) are quantified biochemically and integrated into a general stress indicator. Energy consumption is estimated by measuring the electron transport activity (ETS) at the mitochondrial level, while the energy reserve available for metabolism is assessed by measuring the total lipid, protein and sugar content. Moreover, the difference between E_a and E_c represents the net energy budget of the test organism (De Coen and Janssen, 1997).

In addition, ETS activity is commonly used as a measure of the potential respiration that could be supported by the enzymatic machinery activity (Freitas et al. 2020a). In this sense, an increase of the total protein (PROT) content may result from higher production of enzymes, namely antioxidant enzymes, to fight against the stress induced (Freitas et al. 2020a). Organisms under stressful conditions may increase their metabolic capacity to fuel up defence mechanisms. Accompanying this increased metabolism, the expenditure of energy reserves can also increase, leading to a decrease on organism's protein, glycogen and lipids content. Nevertheless, under low stress levels organisms may be able to decrease their metabolism to avoid accumulation of pollutants (example: bivalves close their valves and reduce filtration rate), leading to accumulation of energy reserves. On the other hand, under high stress conditions organisms may not be able to increase their metabolic capacity although expenditure of energy reserves can continue (Freitas et al. 2020a).

3.4 Responses of aquatic organisms to Gadolinium

3.4.1 Impacts in Mytillus galloprovincialis

In the study developed by Henriques et al. (2019), a toxicological assessment of anthropogenic gadolinium towards the mussel species *Mytilus galloprovincialis* had been performed using different metal concentrations, namely 15, 30, 60 and 120 µg/L (see section 3.2.1). Biological responses were assessed using biochemical markers described in section 3.3. For what concerns energy related biomarkers, it has been noted that mussels exposed to Gd significantly decreased their electron transport system (ETS) activity in comparison to non-contaminated ones. ETS values decreased as the Gd concentration increased until an almost constant value was reached for the two highest metal quantities (60 and 120 µg/L). The initial lowering was thought to be a result of a filtration rate reduction to avoid the pollutant accumulation. Nevertheless, since the decrease of ETS was not proportional to the increase of Gd concentrations, it seems plausible that above certain limits of stress, mussels were not able to further decrease their metabolic rate (Henriques et al., 2019). On the contrary, contaminated mussels significantly increased their energy reserves (glycogen content – GLY) and protein content (PROT), in comparison to control organisms, with the highest values found in those exposed to a Gd concentration of 60 µg/L. At the highest exposure concentration (120 µg/L), instead, mussels, even with their metabolic capacity reduced, started to employ their energy reserves. This indicates that at higher stress levels GLY and PROT were probably necessary to fuel up defence mechanisms (Henriques et al., 2019). Moreover, the analysis of *M. galloprovincialis* oxidative stress biomarkers had been performed. In particular, the activity of

superoxide dismutase (SOD) enzyme was significantly higher in mussels exposed to Gd in comparison to control organisms. Also the activity of catalase (CAT) increased in those organisms exposed to the metal contaminant comparatively to control mussels. The activity of glutathione peroxidase (GPx) instead, was significantly higher in organisms exposed to 30 and 60 µg/L in relation to the remaining conditions (CTL, 15 and 120 µg/L) (Henriques et al., 2019). As described in the previous chapters, when organisms are exposed to pollutants an overproduction of reactive oxygen species (ROS) can occur with an associated antioxidant defence response, including the increase of antioxidant enzymes activity such as SOD, CAT and GPx. Thus, the results obtained in this study indicate that mussels increased their antioxidant defence capacity in the presence of Gd, but this response was only effective up to certain limits since the highest enzymes activities were observed at intermediate concentrations (Henriques et al., 2019). Similar responses have been found by Pinto et al. (2019) and by Freitas et al. (2020a) exposing *M. galloprovincialis* to lanthanum (La) and Dysprosium (Dy) pollutants respectively. Both elements caused an increase in SOD, CAT and GPx enzymes activity but a lower electron transport system (ETS) had been found in the former case while a higher ETS has been noted in the latter one.

Results evidenced that at higher stress levels, which means higher Gd concentration (60 and 120 µg/L), mussels were not able to proportionally increase their antioxidant capacity, showing enzyme activities similar to control levels (Henriques et al., 2019). Such behaviour may indicate that the overproduction of ROS caused the inhibition of the activity of these enzymes. Another possible answer could be that organisms were capable of developing other defence mechanisms that prevent Gd toxicity and there was no need for higher antioxidant defence (Henriques et al., 2019). However, any proof regarding this latter hypothesis have been found employing the present biomarkers as indicators of oxidative stress.

For what concerns glutathione-S-transferases (GSTs) enzymes, their activity was significantly higher in organisms exposed to Gd in comparison to control values. As for the antioxidant enzymes, the results obtained indicate that at higher Gd exposure concentrations mussels were no longer able to continue to increase the activity of GSTs enzymes along with the increase of Gd.

Moreover, lipid peroxidation (LPO) levels were significantly higher in mussels exposed to Gd pollutant in comparison to mussels under CTL condition. In addition, organisms exposed to Gd showed significantly lower GSH/ GSSG values comparatively to control values, with no significant differences among Gd exposure conditions (15, 30, 60 and 120 µg/L) (Henriques et al., 2019). These findings clearly demonstrated that Gd induced cellular damage in mussels exposed to this element,

which were accompanied by an oxidative status evidenced by low GSH/GSSG values (Henriques et al., 2019).

3.4.2 Impacts in Dresissena polymorpha

Hanana et al. (2017) investigated the response of zebra mussel, *Dresissena polymorpha*, collected in Saint-Laurence river, Quebéc, Canada, to $GdCl_3$ and its pharmaceutical form gadodiamide (Omniscan). For this purpose, mussels' responses at the transcriptional level of several genes involved in diverse pathways were assessed: *SOD* and *CAT* – protection against oxidative stress; metal and xenobiotic detoxification; *MT* and *GST* - mitochondrial alterations; LPO - lipid damage; DNA damage; GST and inflammation. Mussels were exposed to increasing concentrations of $GdCl_3$ and Omnsican (namely 10, 50, 250 and 1250 µg/L) for 28 days (data on bioaccumulation shown in section 3.2.3). At the highest concentration (1250 µg/L), $GdCl_3$ induced an increase of *SOD* mRNA levels while decreasing the *CAT* ones. This caused an upregulation of superoxide dismutase and a downregulation of catalase enzymes with a consequent production of H_2O_2 (Hanana et al., 2017). These data are in accordance with previous studies, which indicated that $GdCl_3$ was able to promote cell apoptosis due to an increase of reactive oxygen species (ROS) production (Liu et al., 2003; Xia et al., 2011; Ye et al., 2011). Moreover, since ROS are known to induce DNA damage and no genotoxic effects have been noticed in the organism after $GdCl_3$ exposure, Hanana et al. (2017) suggested that the modulation in the expression of *SOD* and *CAT* genes, were able to limit ROS formation and thus DNA and lipidic damages (Hanana et al., 2017). Thanks to these changings, *D. polymorpha* was able to establish an oxidative stress homeostasis, thus preventing any tissue or DNA damages, since no alteration of LPO levels have been reported (Figure 13 A). Another manifestation of the stress induced by Gd treatment was the modulation of the expression of metallothionein (MT) proteins which are known to play a role in the detoxification of metals and in the ROS scavenging. Nevertheless, the pathways involved in *MT* gene modulation are not completely clear (Hidalgo et al., 1988; Wong et al., 2004; Hassinen et al., 2010). For this reason, further researches must be performed in this sense. Also, *GSTs* gene expression was downregulated with the highest Gd exposure concentration, but its enzymatic activity was not significantly affected (Hanana et al., 2017). The lack of a noticeable effect on GST activity could be due to the blocking of common steps in the expression of the detoxifying enzymes by $GdCl_3$ through the competitive inhibition of intracellular calcium influx (Kim and Choi,1997).

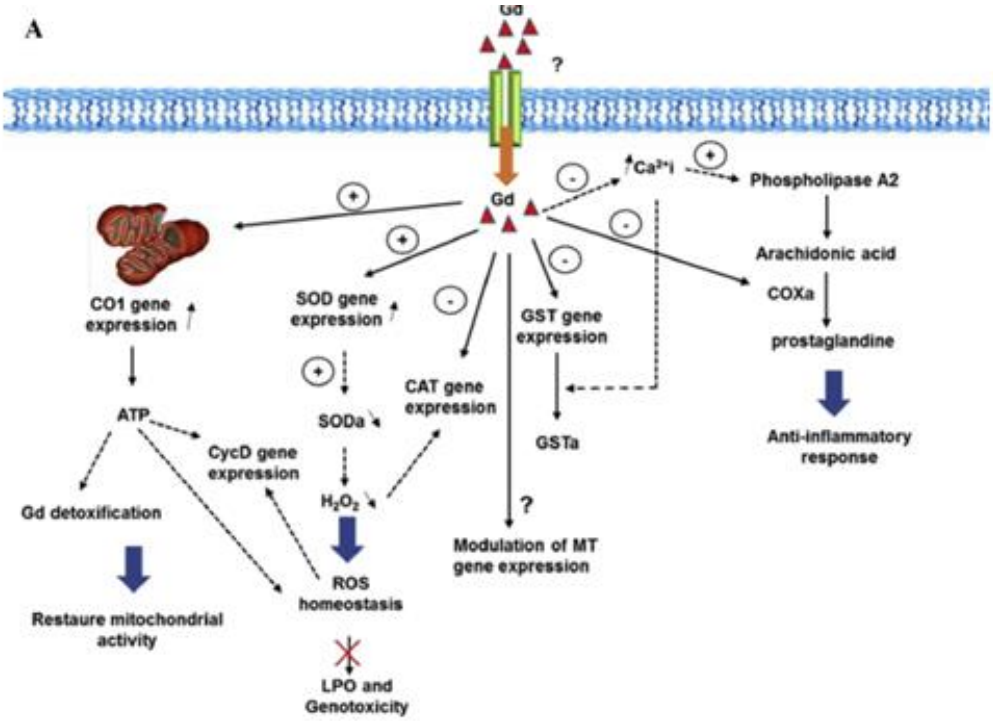

***Figure 13-A**- Scheme of different pathways involved in the mechanism of action of gadolinium (GdCl3). Hypothetical pathways and results obtained in this study are represented by dotted and continued arrows, respectively. SOD: superoxide dismutase, CAT: catalase, CO1: cytochrome c oxidase 1, GST: glutathione S-transferase, Cyc D: cyclin D, MT: metallothioneins, LPO: lipid peroxidation, COXa: cyclooxygenase activity and GSTa: GST activity (Hanana et al., 2017*).

In addition, this study revealed an overexpression of the cytochrome c oxidase (*CO1*) gene, which caused a higher metabolic activity at the electron transport system (ETS) level. This consequently led to an overproduction of ATP. Chalghmi et al. (2016) and Karray et al. (2015) proposed that this mechanism could have been activated in order to compensate the decreased mitochondrial activity. Therefore, a higher production of ATP molecules could be a cellular strategy to provide enough energy for metal detoxification. Finally, in order to elucidate the role played by Gd in the induction of inflammatory response, cyclooxygenase (COX) activity was measured. The high negative relationship found between COX activity and the Gd level in the tissue suggested that Gd plays also an anti-inflammatory role (Hanana et al., 2017).

Analysis performed employing Omniscan showed that this GBCA induced a slight decrease in *SOD*, *CAT* and *GST* gene expression, but no correlation has been found with Gd concentration in tissues. Similarly, to what had been found for the gadolinium salt, a positive relationship has been observed between those genes and the mRNA level of the *CO1* gene which was downregulated in organisms exposed to Omniscan. Therefore, also in this case seems that the activity of *CO1* gene is involved in ROS homeostasis. The downregulation of *SOD* and *CAT* instead, could be due to the antioxidative behaviour of Omniscan, which causes the natural mechanisms of the cells to be expressed to a lower

extent (Figure 13 B) (Hanana et al., 2017). The increase in antioxidant capacity and ROS scavenging activity is responsible of a reduction of the physiological deterioration (Yin et al., 2008).

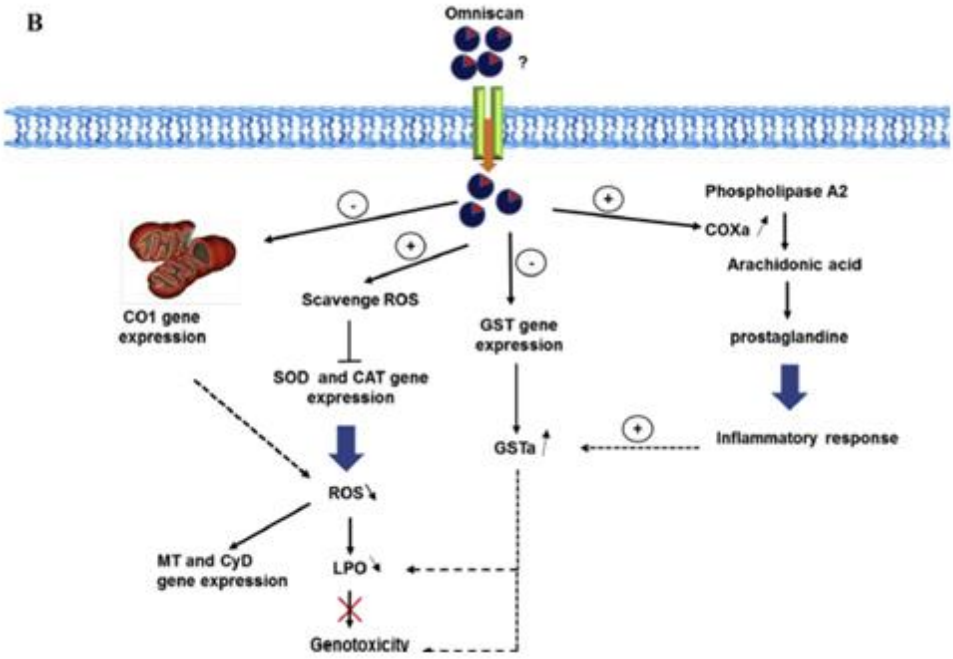

Figure 13-B - Scheme of different pathways involved in the mechanism of action of Omniscan. Hypothetical pathways and results obtained in this study are represented by dotted and continued arrows, respectively. SOD: superoxide dismutase, CAT: catalase, *COXa: cyclooxygenase activity and GSTa: GST activity (Hanana et al., 2017*).

Nevertheless, no tissue damage has been observed as revealed by the significant decrease of LPO level. This was a further insight on the fact that Omniscan did not promote ROS production and may exhibit antioxidant protective activity in mussels exposed *in vivo* (Hanana et al., 2017). Further studies focused on DNA expression, determined that also Omniscan did not induce a genotoxic effect.

Therefore, from the results obtained in Hanana et al. (2017) article, it is possible to determine that the chelated Gd does not act as a biologically inert compound as usually thought (Wermuth et al., 2012). It must be said, finally, as can be seen by Figures 13 A and 13 B, that no insight about any possible Gd uptake mechanism have been determined in this article for both $GdCl_3$ and Omniscan compounds. In addition, some of the metabolic correlations caused by Gd pollutants exposure have not been demonstrated by precise data and are only hypothetical pathways suggested by authors (dotted lines Figure 13 A, 13 B). This is a further demonstration of the lack of information present in literature about this emerging contaminant. For these reasons, further researches must be performed in this sense, in order to better understand the biochemical pathway of these pollutants in different marine and freshwater organisms.

3.4.3 Impacts in Dreissena rostriformis bugensis and Corbicula fluminea

Perrat et al. (2017) studied the effects of gadolinium pollutant in the form of gadoteric acid (Gd-DOTA - Dotarem) in two freshwater bivalves species, namely *Dreissena rostriformis bugensis* and *Corbicula fluminea* organisms, with reference to Gd bioaccumulation (see sections 3.2.2 and 3.3.2). Biochemical biomarkers such as acid phosphatase (ACP), glutathione peroxidase (GPx), lactate dehydrogenase (LDH), lipid peroxidation (LPO) , glutathione-S-transferases (GSTs), electron transport system attached to the mitochondria (ETS), catalase (CAT), and the total antioxidant capacity (TAC) have been measured. Nevertheless, no variation of enzymes activities was observed when compared to controls neither after a 21-day exposure in the presence of 1 or 10 µg/L nor after a 7-day exposure in the presence of 1 µg/L of Gd-DOTA (Perrat et al., 2017). These results are in accordance with those reported by Hanana et al. (2017) and Henriques et. al (2019), in whose experiments, no Gd bioaccumulation had been detected in bivalve species when exposed to a so low metal concentration. On the other hand, after a 7-day exposure to 10 µg/L of pollutant, a significant increase of glutathione S-transferase (GST) activity compared to controls have been observed in the digestive gland of *D. rostriformis bugensis* while an increase in lipid hydroperoxide (LPO) and mitochondrial electron transfer system (ETS) has been observed in the digestive gland of *C. fluminea*. These variations suggested a transient response in both organisms with a faster response in *D. rostriformis bugensis*. Indeed, the response (GST activity increase) persisted in *D. rostriformis bugensis* after 7 days of exposure suggesting an early suppression of any effects. In the case of *C. fluminea*, a proof of toxicity (lipid peroxidation) and an increase in energy expenditure (mitochondrial electron transfer system) were observed after a 7-day exposure but disappeared after a 21-day one (Perrat et al., 2017). Moreover, all biomarkers displayed a basic value at 21 days of exposure, suggesting a response and the deletion of toxic effects between 7 and 21 days of exposure in the digestive gland of *C. fluminea*. All these responses in the digestive gland of *D. rostriformis bugensis* and *C. fluminea* were supposed to be a consequence of the substantial bioaccumulation in this tissue (Perrat et al., 2017). As for the biochemical activities in the gills, no significant variations were observed during the experiments. These results agree with the previous data of Perrat et al. (2017) (see sections 3.2.2 and 3.3.2) which displayed a low bioaccumulation of Gd in the gills tissue. This could mean that the first defence mechanism in the organism acts to expel xenobiotics out of the cell. In this way, the bioaccumulation of Gd is limited, minimizing cell toxicity and therefore biochemical responses (Perrat et al., 2017). This remain a hypothesis, since no specific pathways for any of the free REEs ions have been described so far in literature.

Summing up, this experiment showed that Gd bioaccumulation can induce some responses, i.e, an induction of GST activity, lipid hydroperoxide, and mitochondrial electron transfer system, but a return to the basic activities is observed within 21 days of exposure. This observation is characteristic of a biochemical acclimation to the presence of a pollutant. In addition, these findings suggest that Gd-CAs could accumulate in the tissues of bivalves without any diseases at that moment but there are no further insights about, how long will Gd-CAs stay unmodified after bioaccumulation and if it could be released in the organisms' tissues. Further researches should be performed in order to observe the bioaccumulation for more than 21 days of exposure to assess if a stability could be achieved after longer exposure periods (Perrat et al., 2017).

3.4.4 Impacts in skeleton development of sea urchins

Martino et al. (2018) investigated the potential alterations caused by dissolved gadolinium ion to the skeleton formation mechanism in two species of sea urchin, namely *Paracentrotus lividus* and *Haliotis tubercolata.* Gadolinium Acetate Tetrahydrate (GAT) has been employed as a source of Gd and different concentrations have been used: 20 µM for *P. lividus*; 500 nM and 5 µM for *H. tuberculate.* These marine organisms obtain Ca^{2+} from seawater which is then employed in the construction of the skeleton and spicules. Skeletogenesis is initiated during the early embryonic stage by the so called "primary mesenchyme cells" (PMCs), which have been thought to possess active transporters with high capacity and low affinity, even if they have not yet been identified (Martino et al., 2018). Due to the similarity between Gd^{3+} and Ca^{2+} ionic radii, the gadolinium cation present in the environment could be uptake instead of the calcium one, causing malformation of the skeleton (Sherry et al., 2009). *P. lividus* and *H. tuberculata* exhibited a similar morphological response to Gd. The first effects of Gd were visible at the gastrula stage (24 hours post fertilization - hpf), at the beginning of skeletogenesis, in which Gd-exposed embryos lacked spicules. It appears that Gd-exposure mainly affected skeleton formation in both species, resulting in a range of abnormalities with a severe inhibition of skeleton growth and patterning in treated embryos (Martino et al., 2018). Some embryos had shorter spicules leading to a reduction of arm length, while others had an asymmetric skeletal pattern. To investigate the relationship between Gd exposure, Ca^{2+} uptake and skeleton growth, Ca^{2+} and Gd^{3+} content have been analysed by FAAS. From the data obtained it could be noted that control *P. lividus* embryos showed a 10-fold higher total amount of Ca at 48 hpf than at 24 hpf. This meant that Ca^{2+} was being employed for the skeleton development. On the contrary, in Gd-treated embryos, a 45.54% and 78.81% reduction in the amount of calcium compared to controls has been noted at 24 hpf and at 48 hpf, respectively.

The increase in Ca^{2+} levels during development in Gd-exposed embryos was weak if compared to controls. No Gd was detectable in controls while Gd-exposed embryos had 427.8 ng/mg ± 60 at 24 hpf and 674.66 ng/mg ± 49 at 48 hpf (Martino et al., 2018). Gadolinium-exposed *H. tuberculata* embryos instead, showed an 80% and 90% reduction in the amount of calcium at both concentrations at 24 hpf and at 48 hpf, respectively. Thus, the lowest Gd concentration tested (500 nM) was sufficient to block calcium uptake. These results are in accordance with those obtained by Gravina et al. (2018) where $GdCl_3$ exposure, in concentration ranging between 10^{-7} and 10^{-5} M, resulted in significant damage to embryogenesis and inhibition of fertilization success in *P. lividus*, *Arbacia lixula* and *Sphaerechinus granularis* (Gravina et al., 2018; Oral et al., 2017).

In addition, altered expression of genes associated with skeletogenesis have been reported (Martino et al., 2018). These experiments enlightened that gadolinium exposure has a negative effect on skeleton development and embryogenesis with a similar morphological response in the species tested, implying a similar mechanism underlying these malformations (Martino et al., 2018). Finally, the disruption of spicule formation is likely to be due to the action of Gd^{3+} as a blocker of calcium channels. In fact, being Gd^{3+} a trivalent ion, it is able to bind with a much higher affinity compared to the divalent calcium cation (Sherry et al., 2009). These results are in accordance with other literature papers, which have found similar data, employing different invertebrate species (Kim and Choi, 1997; Hanana et al., 2017).

4. Conclusions and future perspectives

Gadolinium is one of the most commercially exploited REEs which finds it major application in the biomedical field as contrast agent in magnetic resonance imaging (MRI) after chelating it with either macrocyclic or linear organic molecules (Runge, 2018). Even if its complexation almost cancels the toxicity of this metal, many articles suggest that gadolinium complexes may cause the appearance of severe diseases such as nephrogenic system fibrosis (NSF), mostly in those patients suffering from kidney failure (Grobner and Prischl, 2007; Mendichovszky et al., 2007; Clases et al., 2018; Henriques et al., 2019). At the cellular level, Gd toxicity is displayed when metal atoms are present in their free form as positively charged ions Gd^{3+}. Due to the similarity of this ion with the calcium one, free gadolinium behaves as an inorganic blocker of many types of voltage-gated Ca^{2+} channels, causing alterations in the cellular balance (Sherry et al., 2009). In addition, it inhibits physiological processes which depend upon calcium influx, causing lack in contraction of smooth, skeletal and cardiac muscles, transmission of nervous influx or blood coagulation, as well as the activity of some enzymes (Bellin and Van Der Molen, 2008; Rogowska et al., 2018).

Its wide employment enhances the risk for this element to be potentially released into the environment, in particular into rivers, lakes and coastal areas through industrial wastewaters or through exhausted devices (Bau and Dulski, 1996; Kulaksız and Bau, 2011; Hatje et al., 2016; Khan et al., 2017). The highest freshwaters Gd values reported have been found in Germany (Kummerer and Helmers, 2000; Kulaksiz and Bau, 2007), France (particularly the Lorraine region) (Rabiet, 2009; Parant et al., 2018; Pereto et al., 2020) and Turkey (Alkan et al., 2020), with concentrations reaching 30.1, 80 and 0.347 µg/L respectively. Gd anomalies have been also found in China (Zhao et al. 2007; Zhou et al. 2012; Wang et al., 2019), Brazil (De Campos and Enzweiler, 2016; Pedreira et al., 2018) and USA (Barber et al., 2015; Hatje et al., 2016; Altomare et al., 2020), principally in WWTPs effluents, river and coastal waters near hospitals and small clinics. Nevertheless, no specific data concerning anthropogenic Gd concentrations in marine and freshwaters have been reported in Chinese and Brazilian articles. Concerning marine waters instead, very few informations are present in literature. This is mainly due to the high difficulty in determining REEs in seawater due to the remarkable matrix effect and potential spectral interferences during measurement with spectrometers (ICP-MS) (Pyrzynska et al., 2016). Another obstacle in this sense is the difficulty in the differentiation of the background concentration, due to the geogenic processes present in water. This fact could therefore cause high oscillations in the analytical data obtained. Another aspect that must be pointed out is that the highest Gd anomalies were found in the most

industrialized and densely populated areas, which are those possessing the highest number of medical facilities. This is the proof that Gd can be considered as an indicator for the monitoring of anthropogenic pollution.

Nevertheless, limited information is available about Gd biochemical and physiological effects in aquatic organisms. In the articles presented in this thesis, a wide variety of marine and freshwater invertebrates have been considered, with a consequent high differentiation among the toxic responses. It seems clear from the data collected from the literature, that Gd is bioaccumulated by organisms in a different extent, according to its speciation in water. In fact, chelated gadolinium-based contrast agents (GBCAs) used in medical field, display a lower bioavailability compared to free Gd forms, due to their high stability in aquatic environment (Le Goff et al., 2019). In accordance with this, higher bioaccumulation in organisms' tissues and more intense effects on the oxidative homeostasis have been detected employing free Gd ions, compared to complexed compounds in all the species tested (Hanana et al., 2017; Perrat et al., 2017). For these reasons, in all the *in-situ* exposition experiments (Perrat et al., 2017; Pereto et al., 2018), where a higher Gd^{3+} concentration was present due to geogenic processes, a more pronounced bioaccumulation in the organisms tested (namely *Dreissena rostriformis bugensis* and *Corbicula fluminea*) have been reported. Values ranged from 86 to 223 ng/g for *D. rostriformis bugensis* and from 6 to 65 ng/g for *C. fluminea*.

Nevertheless, GBCAs, at the beginning considered as inert, displayed many biochemical and physiological anomalies in all the organisms tested. For example, laboratory experiments performed by Hanana et al. (2017), showed that the GBCA Omniscan caused a downregulation of *SOD*, *CAT*, *CO1* and *GST* genes in *D. polymorpha* even if it was low accumulated in the organism's tissue. Nevertheless, no tissue and DNA damages have been observed as revealed by the significant decrease of LPO level. This was a further insight on the fact that Omniscan did not promote ROS production and may exhibit antioxidant protective activity in mussels exposed *in vivo*. In addition, Le Goff et al. (2019) and Martino et al. (2018) showed that Gd can also be bioaccumulated in *P. maximus* shells and employed in the skeleton and spicule formation in *P. lividus* and *H. tuberculata* seawater urchins, causing skeletal aberrations in the latter case. However, even if nowadays the production and the employment of GBCAs is much higher compared to the past, smaller Gd anomalies in *P. maximus* shell have been recorded (Le Goff et al., 2019). This can be interpreted as a further proof of the lower bioavailability of these compounds due to their high stability in water.

Another gadolinium-based contrast agent, Dotarem (Gd-DOTA) has been tested on two bivalve species (*D. rostriformis burgensis* and *C. fluminea*) by Perrat et al. (2017). Results obtained showed

that this complex can bioaccumulate in the digestive glands, causing an induction of GSTs, LPO and ETS in these tissues. However, after 21 days a return to basic conditions has been noted, evidencing an acclimation of both organisms.

These studies evidenced only few responses considering a small amount of aquatic invertebrate species, meaning that further researches must be performed in order to better understand the absorption mechanism of Gd pollutants and how they behave in organisms' tissues. In fact, little is known about the possible modifications that these complexes can undergo after accumulation. In some cases, a release of toxic Gd ions into organisms' tissues could happen. In addition, particular efforts must be done in understanding the long-term GBCAs stability in marine and freshwater environments, since their production and consequently their discharge through WWTPs is increasing every year.

5. References

Achard M., Baudrimont M., Boudou A., Bourdineaud J. P.; Induction of a multixenobiotic resistance protein (MXR) in the Asiatic clam *Corbicula fulminea* after heavy metal exposure; *Aquatic Toxicology*; **2004**; 67(4); 347-357.

Alkan, A. Alkan, N. Yanar, B; Investigation of pollution levels originated from anthropogenic gadolinium in Ankara Stream; *Environmental Science and Pollution Research*; **2020**.

Alomari E., Bruno S., Ronda L., Paredi G., Bettati S., Mozzarelli A.; Protein carbonylation detection methods: A comparison; *Data in Brief*; **2018**; 19; 2215-2220.

Alpert A. J.; Hydrophilic-interaction chromatography for the separation of peptides, nucleic acids and other polar compounds; *Journal of Chromatography A*; **1990**; 499; 177-196.

Altomare A. J., Young N. A., Beazley M. J.; A preliminary survey of anthropogenic gadolinium in water and sediment of a constructed wetland; *Journal of Environmental Management*; **2020**; 255.

Ammann A. A.; Inductively coupled plasma mass spectrometry (ICP-MS): a versatile tool; *Journal of Mass Spectrometry*; **2007**; 42; 419-427.

Anastopoulos I., Bhatnagar A., Lima E. C.; Adsorption of rare earth metals: A review of recent literature; *Journal of Molecular Liquids*; **2016**; 221; 954-962.

Atwood D. A.; The Rare Earth Elements. Fundamentals and Applications; *John Wiley & Sons, West Sussex*; **2012**.

Augusto F., Hantao L.W., Mogollón G.S., Braga S.C.G.; New materials and trends in sorbents for solid-phase extraction; *Trends in Analytical Chemistry*; **2013**; 43; 14-23.

Baedecker P. A.; Methods for Geochemical Analysis; *U.S. Geological Survey Bulletin*; **1770**.

Balusamy B., Taştan B. E., Ergen S. F., Uyarbe T., Tekinay T.; Toxicity of lanthanum oxide (La2O3) nanoparticles in aquatic environments; *Environmental Science: Processes & Impacts*; **2015**; 17; 1265-1270.

Barber L. B., Loyo-Rosales J. E., Rice C. P., Minarik T. A., Oskouie A. K., Endocrine disrupting alkylphenolic chemicals and other contaminants in wastewater treatment plant effluents, urban streams, and fish in the Great Lakes and Upper Mississippi River Regions; *Science of the Total Environment*; **2015**; 517; 195-206.

Bau M., Dulski P.; Anthropogenic origin of positive gadolinium anomalies in river waters; *Earth and Planetary Science Letters*; **1996**; 143(1-4); 245-255.

Bellin M., Van Der Molen A. J.; Extracellular gadolinium-based contrast media: An overview; *European Journal of Radiology*; **2008**; 66; 160–167.

Birka M., Roscher J., Holtkamp M., Sperling M., Karst U.; Investigating the stability of gadolinium based contrast agents towards UV radiation; *Water Research*; **2016**; 91; 244-250 (b).

Birka M., Wehe C. A., Hachmoller O., Sperling M.; Tracing gadolinium-based contrast agents from surface water to drinking water by means of speciation analysis; *Journal of Chromatography A*; **2016**; 1440; 105-111 (a).

Blaise C., Gagne F., Harvood M., Quinn B., Hanana H.; Ecotoxicity responses of the freshwater cnidarian *Hydra attenuata* to 11 rare earth elements; *Ecotoxicology and Environmental Safety*; **2018**; 163; 486-491.

Blinova I., Lukjanova A., Muna M., Vija H., Kahru A.; Evaluation of the potential hazard of lanthanides to freshwater microcrustaceans; *Science of The Total Environment*; **2018**; 642; 1100–1107.

Braun M., Zavanyi G., Laczovics A., Berényi E., Szabó S.; Can aquatic macrophytes be biofilters for gadolinium based contrasting agents?; *Water Research*; **2017**.

Byrne R.H., Liu X.W., Schijf J.; The influence of phosphate coprecipitation on rare earth distributions in natural waters; *Geochimica et Cosmochimica Acta*; **1996**; 60; 3341–3346.

Chakhmouradlan A. R., Wall F.; Rare earth elements: Minerals, Mines, Magnets; *Elements*; **2012**; 8; 333–340.

Chalghmi H., Bourdineaud J. P., Haouas Z., Gourves P. Y., Zrafi I., Saidane-Mosbahi D.; Transcriptomic, biochemical, and histopathological responses of the clam ruditapes decussatus from a metal-contaminated tunis lagoon; *Archives of Environmental Contamination and Toxicology*; **2016**; 70; 241-256.

Cheremisinoff N. P.; Polymer Characterization; *Laboratory Techniques and Analysis*; **1996**; 43-81.

Chiesa S., Azzurro E., Bernardi G.; The genetics and genomics of marine fish invasions: a global review; *Reviews in Fish Biology and Fisheries*; **2019**; 29; 837–859.

Clases D., Sperling M., Karst U.; Analysis on metal-based contrast agents in medicine and the environment; *Trends in Analytical Chemistry*; **2018**; 104; 135-147.

Coppola F., Almeida A., Henriques B., Soares A. M. V. M., Figueira E., Pereira E., Freitas R.; Biochemical responses and accumulation patterns of *Mytilus galloprovincialis* exposed to thermal stress and Arsenic contamination; *Ecotoxicology and Environmental Safety*; **2018**; 147; 954-962.

Cyris M.; Behavior of Gadolinium-based Diagnostics in Water Treatment; **2013**.

D'Aquino L., Morgana M., Carboni M. A., Staiano M., Antisari M. V., Re M., Lorito M., Vinale F., Abadi K. M., Woo S. L.; Effect of some rare earth elements on the growth and lanthanide

accumulation in different *Trichoderma* strains; *Soil Biology and Biochemistry*; **2009**; 41(12); 2406-2413.

De Coen W.M., Janssen C.R., Persoone G.; Biochemical assessment of Cellular Energy Allocation in Daphnia magna exposed to toxic stress as an alternative to the conventional "Scope for Growth" methodology; *Proceedings International Symposium on Biological Markers of Pollution*; **1995**; 21–22; 163–170.

De Coen W.M., Janssen C.R.; The use of biomarkers in Daphnia magna toxicity testing. IV. Cellular Energy Allocation: a new methodology to assess the energy budget of toxicant-stressed Daphnia populations; *Journal of Aquatic Ecosystem Stress and Recovery*; **1997**; 6; 43–55.

Duarte B., Caçador I.; Ecotoxicology of marine organisms; *CRC Press*; **2020**.

Emsley J.; Nature's Building Blocks: An A–Z Guide to the Elements; *Oxford University Press, New York, NY, USA*; **2011**.

Fernández B., Lobo L., Pereiro R.; Atomic Absorption Spectrometry|Fundamentals, Instrumentation and Capabilities; *Molecular Sciences and Chemical engineering*; **2019**; 137-143.

Ferreira de Campos F., Enzweiler J.; Anthropogenic gadolinium anomalies and rare earth elements in the water of Atibaia River and Anhumas Creek, Southeast Brazil; *Environmental Monitoring and Assessment*; **2016**; 188 (281).

Freitas R., Cardoso C. E. D., Costa S., Morais T., Moleiro P., Lima A. F.D., Soares M., Figueiredo S., Agueda T. L., Rocha P., Amador G., Soares A.M.V.M., Pereira E.; New insights on the impacts of e-waste towards marine bivalves: The case of the rare earth element Dysprosium; *Environmental Pollution*; **2020**; 260; 113859) (a).

Freitas R., Costa S., Cardoso C. E. D., Morais T., Moleiro P., Matias A., C., Pereira A. F., Machado J., Correia B., Pinheiro D., Rodrigues A., Colónia J., Soares A. M. V. M., Pereira E.; Toxicological effects of the rare earth element neodymium in *Mytilus galloprovincialis*; *Chemosphere*; **2020**; 244; 125457 (b).

Fujiwara K., Matsumoto Y., Kawakami H., Aoki M., Tuzuki M.; Evaluation of Metal Toxicity in Chlorella kessleri from the Perspective of the Periodic Table; *Bulletin of the Chemical Society of Japan*; **2008**; 81 (4); 478-488.

Gama M. R., Da Costa Silva R. G., Collins C. H., Bottoli C. B. G.; Hydrophilic interaction chromatography; *Trends in Analytical Chemistry*; **2012**; 37; 48-60.

Gilstrap R., Allen R.; A colloidal nanoparticle form of indium tin oxide: system development and characterization; *Georgia Institute of Technology*; **2009**.

Gonzalez V., Vignati D. A. L., Leyval C., Giamberini L., Environmental fate and ecotoxicity of lanthanides: Are they a uniform group beyond chemistry?; *Environment International*; **2014**; 71; 148-157.

González V., Vignati D. A. L., Pons M., Montarges-Pelletier E., Bojic C., Giamberini L.; Lanthanide ecotoxicity: First attempt to measure environmental risk for aquatic organisms; *Environmental Pollution*; **2015**; 199; 139-147.

Goodenough K. M., Schilling J., Jonsson E., Kalvig P., Charles N., Tuduri J., Deady E. A., Sadeghi M., Schiellerup H., Müller A., Bertrand G., Arvanitidis N., Eliopoulos D. G., Shaw R. A., Thrane K., Keulen N.; Europe's rare earth element resource potential: an overview of REE metallogenetic provinces and their geodynamic setting; *Ore Geology Reviews*; **2016**;72, 838–856.

Graney Jr R. L., Cherry D. S., Cairns Jr J.; The influence of substrate, pH, diet and temperature upon cadmium accumulation in the asiatic clam (*Corbicula fulminea*) in laboratory artificial streams; *Water Research*; **1984**; 18 (7); 833-842.

Gravina M., Pagano G., Oral R., Giuda M., Toscanesi M., Siciliano A., Di Nunzio A., Buric P., Lyons D. M., Thomas P. J., Trifuoggi M.; Heavy Rare Earth Elements Affect Sphaerechinus granularis Sea Urchin Early Life Stages by Multiple Toxicity Endpoints; *Bulletin of Environmental Contamination and Toxicology*; **2018**; 100; 641–646.

Greenwood A., Norman N., Earnshaw A.; Chemistry of the Elements (2nd ed.), *Butterworth-Heinemann*; **1997**.

Grobner T., Prischl F. C.; Gadolinium and nephrogenic systemic fibrosis; *Kidney International*; **2007**; 72 (3); 260-264.

Grobner T.; Gadolinium: a specific trigger for the development of nephrogenic fibrosing dermopathy and nephrogenic systemic fibrosis? *Nephrology Dialysis Transplantation;* **2005***;* 21, 1104–1108.

Gwenzi W., Mangori L., Danha C., Chaukura N., Dunjana N., Sanganyadoe E.; Sources, behaviour, and environmental and human health risks of high technology rare earth elements as emerging contaminants; *Science of the Total Environment*; **2018**; 636; 299-313.

Hall G. E. M., Vaive J. E., Beer R., Hoashi M.; Selective leaches revisited, with emphasis on the amorphous Fe oxyhydroxide phase extraction; *Journal of Geochemical Exploration*; **1996**; 56(1); 59-78.

Hanana H., Turcotte P., André C., Gagnon C., Gagné F.; Comparative study of the effects of gadolinium chloride and gadolinium e based magnetic resonance imaging contrast agent on freshwater mussel, *Dreissena polymorpha*; *Chemosphere*; **2017**; 181; 197-207.

Hao S., Xiaorong W., Liansheng W., Lemei D., Zhong L., Yijun C.; Bioconcentration of Rare Earth Elements lanthanum, gadolinium and yttrium in algae (*Chlorella Vulgarize Beijerinck*): Influence of chemical species; *Chemosphere*; **1997**; 34 (8); 1753-1760.

Hassinen V. H., Tervahauta A. I., Schat H., Kärenlampi S. O.; Plant metallothioneins – metal chelators with ROS scavenging activity?; *Plant Biology*; **2011**; 13; 225-232.

Hatje V., Bruland K. W., Flegal A. R.; Increases in Anthropogenic Gadolinium Anomalies and Rare Earth Element Concentrations in San Francisco Bay over a 20 Year Record; *Environmental Science & Technology*; **2016**; 50; 4159−4168.

He M. L., Rambeck W. A.; Rare earth elements-a new generation of of growth promoters for pigs?; *Archives of Animal Nutrition*; **2000**; 53(4); 323-334.

Hemström P., Irgum K.; Hydrophilic interaction chromatography; *Journal of Separation Science*; **2006**; 29(12); 1784-1821.

Henriques B., Coppola F.; Monteiro R., Pinto J., Viana T., Pretti C., Soares A., Freitas R., Pereira E.; Toxicological assessment of anthropogenic Gadolinium in seawater: Biochemical effects in mussels *Mytilus galloprovincialis; Science of the Total Environment*; **2019**; 664; 626-634.

Hidalgo J., Campmany L., Borras M., Garvey J. S., Armario A.; Metallothioneins response to stress in rats: role in free radical scavenging; *American Journal of Physiology-Endocrinology and Metabolism*; **1988**; 255 (4).

Hron T., Kuba J., Cingros F.; Magneto — Caloric effect in gadolinium; *32nd International Spring Seminar on Electronics Technology*, Brno; **2009** 1-4.

Idee J. M., Port M., Raynal I., Schaefer M., Le Greneur S., Corot C.; Clinical and biological consequences of transmetallation induced by contrast agents for magnetic resonance imaging: A review; **2006**; *Fundamental & Clinical Pharmacology*; 20; 563–576.

Joonas E., Aruoja V., Olli K., Syvertsen-Wiig G., Vija H., Kahruad A.; Potency of (doped) rare earth oxide particles and their constituent metals to inhibit algal growth and induce direct toxic effects; *Science of The Total Environment*; **2017**; 593-594; 478-486.

Kamenopoulos S. N., Shields D., Agioutantis Z.; Sustainable development criteria and indicators for the assessment of rare earth element mining projects; *Rare Earths Industry*; **2016**.

Karray S., Tastard E., Moreau B., Delahaut L., Geffard A., Guillon E., Denis F., Hamza-Chaffai A., Chénais B., Marchand J.; Transcriptional response of stress-regulated genes to industrial effluent exposure in the cockle Cerastoderma glaucum; *Environmental Science and Pollution Research*; **2015**; 22; 17303-17316.

Khan A. M., Behkami S., Yusoff I., Md Zain S. B., Bakar N. K. A., Bakar A. F. A., Alias Y.; Geochemical characteristics of rare earth elements in different types of soil: a chemometric approach; *Chemosphere*; **2017**; 184; 673–678.

Khan A. M., Yusoff I., Abu Bakar N. K., Abu Bakar A. F., Alias Y.; Assessing of anthropogenic levels, speciation, and potential mobility of rare earth elements (REEs) in ex-tin mining area; *Environmental Science and Pollution Research*; **2016**; 23; 25039–25055.

Kim S. G., Choi S. H.; Gadolinium chloride inhibition of rat hepatic microsomal epoxide hydrolase and glutathione S-transferase gene expression; *Drug Metabolism and Disposition*; **1997**; 25; 1416-1423.

Kimura J., Hayakari M., Kumano T., Nakano H., Satoh K., Tsuchida S.; Altered glutathione transferase levels in rat skin inflamed due to contact hypersensitivity: induction of the alpha-class subunit 1; *Biochemical Journal*; **1998**; 335; 605-610.

Klinger J. M.; A historical geography of rare earth elements: From discovery to the atomic age; The *Extractive Industries and Society*; **2015**; 2; 572–580.

Klockenkämper R., Von Bohlen A.; Total Reflection X-Ray Fluorescence Analysis and Related Methods; *John Wiley & sons Inc*; **2015**.

Kulaksız S., Bau M.; Anthropogenic dissolved and colloid/ nanoparticle-bound samarium, lanthanum and gadolinium in the Rhine River and the impending destruction of the natural rare earth element distribution in rivers; *Earth and Planetary Science Letters*; **2013**; 362; 43−50.

Kulaksız S., Bau M.; Rare earth elements in the Rhine River, Germany: first case of anthropogenic lanthanum as a dissolved microcontaminant in the hydrosphere; *Environment International*; **2011**; 37; 973-979.

Kulaksız S.; Bau M.; Contrasting behaviour of anthropogenic gadolinium and natural rare earth elements in estuaries and the gadolinium input into the North Sea; *Earth and Planetary Science Letters*; **2007**; 260 (1-2); 361-371.

Kumari A., Panda R., Jha M. K., Kumar J. R., Lee J. Y.; Process development to recover rare earth metals from monazite mineral: A review; *Mineral Engineering*; **2015**; 79; 102-115.

Kummerer K., Helmers E.; Hospital Effluents as a source of Gadolinium in the Aquatic Environment; *Environmental Science & Technology*; **2000**; 34(4); 573-577.

Laurent S., Elst L. V., Muller R. N.; Comparative study of the physicochemical properties of six clinical low molecular weight gadolinium contrast agents; *Contrast Media & Molecular Imaging*; **2006**; 1; 128–137.

Laurent S., Vander Elsta L., Henoumonta C., Mullera R. N.; How to measure the transmetalation of a gadolinium complex; *Contrast Media & Molecular Imaging*; **2010**; 5; 305–308.

Le Goff S., Barrat J., Chauvaud L., Paulet Y., Gueguen B., Salem D. B.; Compound-specific recording of gadolinium pollution in coastal waters by great scallop; *Scientific Report – Nature*; **2019**; 9; 8015.

Levine L. R., Garland D., Oliver C. N., Amici A., Climent I., Lenz A. G., Ahn B. W., Shaltiel S., Stadtman E. R.; [49] Determination of carbonyl content in oxidatively modified proteins; *Methods in Enzymology*; **1990**; 186; 464-478.

Li X., Zhang F., Zhao D.; Highly efficient lanthanide upconverting nanomaterials: Progresses and challenges; *Nano Today*; **2013**; 8; 643–676.

Lindner U., Lingott J., Richter S., Jakubowski N., Panne U.; Speciation of gadolinium in surface water samples and plants by hydrophilic interaction chromatography hyphenated with inductively coupled plasma mass spectrometry; *Analytical and Bioanalytical Chemistry*; **2013**; 405; 1865-1873.

Lingott J., Lindner U., Telgmann L., Esteban-Fernandéz D., Jakubowski N., Panne U.; Gadolinium-uptake by acquatic and terrestrial organism-distribution determined by laser ablation inductively coupled plasma mass spectrometry; *Environmental Sciences: Processes & Impacts*; **2015**.

Liu C., Yang Z., Wang L., Lu Y., Tang B., Miao H., Xu Q., Chen X.; Combination of sorafenib and gadolinium chloride (GdCl3) attenuates dimethylnitrosamine(DMN)-induced liver fibrosis in rats; *BMC Gastroenterology*; **2015**; 15; 159.

Manchen N. A., Sprecher B., Bailey G., Ge J., Tukker A.; Effect of Chinese policies on rare earth supply chain resilience; *Resources Conservation & Recycling*; **2019**;142; 101–112.

Marckmann P.; Nephrogenic systemic fibrosis: suspected causative role of gadodiamide used for contrast-enhanced magnetic resonance imaging; *Journal of the American Society of Nephrology*; **2006**; 17, 2359–2362.

Markich S. J., Jeffree R. A., Burke P. T.; Freshwater Bivalve Shells as Archival Indicators of Metal Pollution from a Copper-Uranium Mine in Tropical Northern Australia; *Journal of the American Chemical Society*; **2002**; 36 (5); 821-832.

Martino C., Costa C., Roccheri M. C., Koop D., Scudiero R., Byrne M.; Gadolinium perturbs expression of skeletogenic genes, calcium uptake and larval development in phylogenetically distant sea urchin species; *Aquatic Toxicology*; **2018**; 194; 57–66.

Mendichovszky I. A., Marks S. D., Simcock C. M., Olsen Ø. E.; Gadolinium and nephrogenic systemic fibrosis: time to tighten practice; *Pediatric Radiology*; **2008**; 38; 489–496.

Merschel G., Bau M.; Rare earth elements in the aragonitic shell of freshwater mussel Corbicula fluminea and the bioavailability of anthropogenic lanthanum, samarium and gadolinium in river water; *Science of the Total Environment*; **2015**; 533; 91-101.

Mestre N. C., Sousa V. S., Rocha T. L., Bebianno M. J.; Ecotoxicity of rare earths in the marine mussel Mytilus galloprovincialis and a preliminary approach to assess environmental risk; *Ecotoxicology*; **2019**; 28; 294–301.

Migaszewski Z. M., Gałuszka A.; The characteristics, occurrence, and geochemical behavior of rare earth elements in the environment: A review; *Critical Reviews in Environmental Science and Technology*; **2015**; 45; 429–471.

Möller P., Morteani G., Dulski P.; Anomalous Gadolinium, Cerium, and Yttrium Contents in the Adige and Isar c o River Waters and in the Water of Their Tributaries (Provinces Trento and Bolzano/Bozen, NE Italy); *Acta hydrochimica et hydrobiologica*; **2003**; 31 (3); 225–239.

Moreira A., Henriques B., Leite C., Libralato G., Pereira E., Freitas R.; Potential impacts of lanthanum and yttrium through embryotoxicity assays with *Crassostrea gigas; Ecological Indicators;* **2020**; 108; 105687.

Normann P. T., Hustvedt S. O., Storflor H., Hals P. A.; Preclinical safety and pharmacokinetic profile of gadodiamide injection; *Clinical MRI*; **1995**; 5; 95-101.

Nozaki Y., Lerche D., Alibo D. S., Snidvongs A.; The estuarine geochemistry of rare earth elements and indium in the Chao Phraya River, Thailand; Geochimica et *Cosmochimica Acta*; **2000**; 64, 3983–3994.

OECD (2015) Health at a glance 2015: OECD indicators, Paris.

Öhrlund, I.; Future Metal Demand from Photovoltaic Cells and Wind Turbines–Investigating the Potential Risk of Disabling a Shift to Renewable Energy Systems; *Science and Technology Options Assessment (STOA), European Parliament*; **2011**.

Oral R., Pagano G., Siciliano A., Gravina M., Palumbo A., Castellano I., Migliaccio O., Thomas P. J., Guida M., Tommasi F., Trifuoggi M.; Heavy rare earth elements affect early life stages in Paracentrotus lividus and Arbacia lixula sea urchins; *Environmental Research*; **2017**; 154; 240–246.

Pagano G., Aliberti F., Giuda M., Oral R., Siciliano A.; Trifuoggi M.; F. Tommasi; Rare earth elements in human and animal health: State of art and research priorities; *Environmental Research*; **2015**; 142; 215-220.

Parant M., Perrat E., Wagner P., Rosin C., Py J., Cossu-Leguille C.; Variations of anthropogenic gadolinium in rivers close to waste water treatment plant discharges; *Environmental Science and Pollution research*; **2018**; 25(36).

Pastorino P., Brizio P., Abete M. C., Bertoli M., Oss Noser A. G., Piazza G., Prearo M., Elia A. C., Pizzul E., Squadrone S.; Macrobenthic invertebrates as tracers of rare earth elements in freshwater watercourses; *Science of the Total Environment*; **2020**; 698.

Pecharsky V. K., Gschneidner Jr. K. A.; Rare-earth element; *Encyclopædia Britannica, inc.*; **2019**.

Pedreira R. M. A., Pahnke K., Böning P., Hatje V.; Tracking hospital effluent-derived gadolinium in Atlantic coastal waters off Brazil; *Water Research*; **2018**; 145; 62-72.

Pereto C., Coynel A., Lerat-Hardy A., Gourves P. Y., Schäfer J., Baudrimont M.; Corbicula fluminea: A sentinel species for urban Rare Earth Element origin; *Science of the Total Environment*; **2020**; 732.

Perrat E., Parant M., Py J. S., Rosin C., Cossu-Leguille C.; Bioaccumulation of gadolinium in freshwater bivalves; *Environmental Science and Pollution Research*; **2017**; 24; 12405–12415.

Pinto J., Costa M., Leite C., Borges C., Coppola F., Henriques B., Monteiro R., Russo T., Di Cosmo A., Soares A. M. V. M., Polese G., Pereira E., Freitas R.; Ecotoxicological effects of lanthanum in *Mytillus galloprovincialis*: Biochemical and histopathological impacts; *Aquatic Toxicology*; **2019**; 211; 181-192.

Pramanik S., Das P.; Nanomaterials and Polymers Nanocomposites; *Elsevier*; **2019**; 91-121.

Pratas J., Favas P. J. C., Varun M., D'Souza R., Paul M. S.; Distribution of rare earth elements, thorium and uranium in streams and aquatic mosses of Central Portugal; *Environmental Earth Sciences*; **2017**; 76; 156.

Pyrzynska K., Kubiak A., Wysocka I.; Application of solid phase extraction procedures for rare earth elements determination in environmental samples; *Talanta*; **2016**; 154; 15-22.

Rabiet M., Brissaud F., Seidel J. L., Pistre S., Elbaz-Poulichet F.; Positive gadolinium anomalies in wastewater treatment plant effluents and aquatic environment in the Hérault watershed (South France); *Chemosphere*; **2009**; 75(8); 1057-1064.

Raju C. S. K., Cossmer A., Scharf H., Panne U., Lück D.; Speciation of gadolinium based MRI contrast agents in environmental water samples using hydrophilic interaction chromatography hyphenated with inductively coupled plasma mass spectrometry; *Journal of Analytical Atomic Spectrometry*; **2010**; 25; 55-61.

Ramalho J., Semelka R. C., Ramalho M., Nunes R. H., AlObaidy M., Castillo M.; Gadolinium-Based Contrast Agents Accumulation and Toxicity: an Update; *American Journal of Neuroradiology*; **2016**; 37; 1192-1198.

Regoli F., Giuliani M. E., Benedetti M., Arukwe A.; Molecular and biochemical biomarkers in environmental monitoring: A comparison of biotransformation and antioxidant defense systems in multiple tissues; *Aquatic Toxicology*; **2011**; 1055; 56-66.

Regoli F., Giuliani M. E.; Oxidative pathways of chemical toxicity and oxidative stress biomarkers in marine organisms; *Marine Environmental Research*; **2014**; 93; 106-117.

Rogowska J., Olkowska E., Ratajczyk W., Wolska L.; Gadolinium as a New Emerging Contaminant of Aquatic Environments; *Environmental Toxicology and Chemistry*; **2018**; 37; 1523-1534.

Runge V. M.; Dechelation (Transmetalation): consequences and safety concerns with the linear gadolinium-based contrast agents, in view of recent Health care rulings by the EMA (Europe), FDA (United States), and PMDA (Japan); *Investigative Radiology*; **2018**; 53(10); 571-578).

Rzymski P., Klimaszyk P., Niedzielski P., Marszelewski W., Borowiak D., Nowiński K., Baikenzheyeva A., Kurmanbayev R., Aladin N.; Pollution with trace elements and rare-earth metals in the lower course of Syr Darya River and Small Aral Sea, Kazakhstan; *Chemosphere*; **2019**; 234; 81-88.

Schijf J., Christy I. J.; Effect of Mg and Ca on the stability of the MRI contrast agent Gd–DTPA in seawater; *Frontiers in Marine Science*; **2018**; 5; 111.

Shen L., Wu N., Zhong S., Gao L.; Overview on China's rare earth industry restructuring and regulation reforms; *Journal of Resources and Ecology*; **2017**; 8; 2013–2022.

Sherry A. D., Caravan P., Lenkinski R. E.; Primer on gadolinium chemistry; *Journal of Magnetic Resonance Imaging*; **2009**; 30; 1240–1248.

Sneller F. E. C., Kalf D. F., Weltje L., Van Wezel A. P.; Maximum permissible concentrations and negligible concentrations for rare earth elements (REEs); Report No. RIVM 601501011; National Institute of Public Health and the Environment, Bilthoven; **2000**.

Taylor S. R., McLennan S. M.; The continental crust: its composition and evolution; *United States, N.p*; **1985**.

Telgmann L., Sperling M., Karst U.; Determination of gadolinium-based MRI contrast agents in biological and Environmental samples: A review; *Analytica Chimica Acta*; **2013**; 764; 1– 16.

Thomsen H. S., Marckmann P.; Extracellular Gd-CA: Differences in presence of NSF; *European Journal of Radiology*; **2008**; 66 (2); 180-183.

Tu R., Kannell T., Turski P., Polzin J., Korosec F., Mistretta C.; Preliminary assessment of Gadodiamide-Enhanced, Complex-Difference Phase-Contrast Magnetic Resonance Angiography; *Academic Radiology*; **1994**; 1; S47-S55.

US-EPA; Rare Earth Elements: A Review of Production, Processing, Recycling, and Associated Environmental Issues; United States Environmental Protection Agency, Cincinnati; OH EPA/600/R-12/572; **2012**.

Verplanck P.L., Taylor H.E., Nordstrom D.K., Barber L.B., Aqueous stability of gadolinium in surface waters receiving sewage treatment plant effluent, boulder creek, Colorado; *Environmental Science and Technology;* **2005**; 39; 6923–6929.

Wang Z., Yin L., Xiang H., Qin X., Wang S.; Accumulation patterns and species-specific characteristics of yttrium and rare earth elements (YREEs) in biological matrices from Maluan Bay, China: Implications for biomonitoring; *Environmental Research*; **2019**; 179.

Wells W. H., Wells V.; The lanthanides, rare earth metals; *Patty's Toxicology (eds E. Bingham, B. Cohrssen and C.H. Powell); New York: Wiley*; **2001**.

Weltje L., Heidenreich H., Zhu W., Wolterbeek H. Th., Korhammer S., De Goeij J. J.M., Markert B.; Lanthanide concentrations in freshwater plants and molluscs, related to those in surface water, pore water and sediment. A case study in The Netherlands; *Science of The Total Environment*; **2002**; 286 (1–3); 191-214.

Wermuth P. J., Jimenez S. A.; Gadolinium Compounds Signaling through TLR 4 and TLR 7 in Normal Human Macrophages: Establishment of a Proinflammatory Phenotype and Implications for the Pathogenesis of Nephrogenic Systemic Fibrosis; *Journal of Immunology*; **2012**; 189 (1); 318-327.

Wong H. L., Sakamoto T., Kawasaki T., Umemura K., Shimamoto K.; Down-Regulation of Metallothionein, a Reactive Oxygen Scavenger, by the Small GTPase OsRac1 in Rice; *Plant Physiology*; **2004**; 135; 1447–1456.

Xia Q., Feng X., Huang H., Du L., Yang X., Wang K.; Gadolinium-induced oxidative stress triggers endoplasmic reticulum stress in rat cortical neurons; *Journal of Neurochemistry*; **2011**; 117; 38–47.

Xu N., Morgan B., Rate A. W.; From source to sink: Rare-earth elements trace the legacy of sulfuric dredge spoils on estuarine sediments; *Science of the Total Environment*; **2018**; 637-638; 1537-1549.

Xun W., Shi L., Hou G., Zhou H., Yue W., Zhang C., Ren Y.; Effect of Rare Earth Elements on Feed Digestibility, Rumen Fermentation, and Purine Derivetives in Sheep; *Italian Journal of Animal Science*; **2014**; 13(2); 357-362.

Ye L., Shi Z., Liu H., Yang X., Wang K.; Gadolinium induced apoptosis of human embryo liver L02 cell line by ROS-mediated AIF pathway; *Journal of Rare Earths*; **2011**; 29 (2); 178-184.

Yessoufou A., Ifon B. E., Suanon F., Dimon B., Sun Q., Dedjiho C. A., Mama D., Yu C.; *Environmental Monitoring and Assessment*; **2017**; 189; 625.

Yin J. J., Lao F., Meng J., Fu P. P., Zhao Y., Xing G., Gao X., Sun B., Wang P. C., Chen C., Liang X. J.; Inhibition of tumor growth by endohedral metallofullerenol nanoparticles optimized as reactive oxygen species scavenger; *Molecular Pharmacology*; **2008**; 74; 1132-1140.

Yu S., Dan'kov A. M., Tishin V. K., Pecharsky, Gschneidner Jr. K. A., Magnetic phase transitions and the magnetothermal properties of gadolinium; *Physical Review*; **1998**; 57(6); 3478-3490.

Zepf V.; An overview of the usefulness and strategic value of rare earth metals. Rare Earths Industry: Technological, Economic, and Environmental Implications; *Elsevier*; **2015**; 3–17.

Zhang P., Zhang L., Tang J.; Lanthanide single molecule magnets: Progress and perspective; *Dalton Transactions*; **2015**; 44; 3923–3929.

Zhang Y., Wei W., Das G. K., Tan T. T. Y.; Engineering lanthanide-based materials for nanomedicine; *Journal of Photochemistry and Photobiology*; **2014**; 20; 71–96.

Zhao F., Cong Z., Sun H., Ren D.; The geochemistry of rare earth elements (REEs) in acid mine drainage from the Sitai coal mine Shanxi Province, North Cina; *International Journal of Coal Geology*; **2007**; 70 (1-3); 184-192.

Zhou B., Li Z., Zhao Y., Zhang C., Wei Y.; Rare earth elements supply vs. clean energy technologies: New problems to be solve; *Gospodarka Surowcami Mineralnymi*; **2016**; 32; 29–44.

Zhou G. H., Sun B. B., Liu Z. Y., Wei H. L., Zeng D. M., Zhang B. M.; Geochemical feature of rare earth elements in major rivers of eastern China; *Geosciences*; **2012**; 26; 1028–104.